



# **10<sup>TH</sup> International Conference on Sustainable Energy and Environmental Protection: Combined and Hybrid Energy Systems**

**(June 27<sup>TH</sup> - 30<sup>TH</sup>, 2017, Bled, Slovenia)**

(Conference Proceedings)

## **Editors:**

Emeritus Prof. dr. Jurij Krope  
Prof. dr. Abdul Ghani Olabi  
Prof. dr. Darko Goričanec  
Prof. dr. Stanislav Božičnik



University of Maribor Press



University of Maribor Press



University of Maribor Press

**10<sup>TH</sup> International Conference on Sustainable Energy and  
Environmental Protection**

**Combined and Hybrid Energy Systems**

**(June 27<sup>TH</sup> – 30<sup>TH</sup>, 2017, Bled, Slovenia)**

**(Conference Proceedings)**

**Editors:**

Emeritus Prof. dr. Jurij Krope

Prof. dr. Abdul Ghani Olabi

Prof. dr. Darko Goričanec

Prof. dr. Stanislav Božičnik

**June 2017**

- Title:** 10<sup>TH</sup> International Conference on Sustainable Energy and Environmental Protection (June 27<sup>TH</sup> – 30<sup>TH</sup>, 2017, Bled, Slovenia) (Conference Proceedings)
- Subtitle:** Combined and Hybrid Energy Systems
- Editors:** Emeritus Prof. Jurij Kroppe, Ph.D. (University of Maribor, Slovenia), Prof. Abdul Ghani Olabi, Ph.D. (University of the West of Scotland, UK), Asso. Prof. Darko Goričanec, Ph.D. (University of Maribor, Slovenia), Asso. Prof. Stanislav Božičnik (University of Maribor, Slovenia).
- Review:** Prof. Željko Knez, Ph.D. (University of Maribor, Slovenia), Prof. Niko Samec, Ph.D. (University of Maribor, Slovenia).
- Technical editors :** Jan Perša (University of Maribor Press), Armin Turanović (University of Maribor Press).
- Design and layout:** University of Maribor Press
- Conference:** 10<sup>TH</sup> International Conference on Sustainable Energy and Environmental Protection
- Honorary Committee:** Abdul Ghani Olabi, Ph.D. (Honorary President, University of the West of Scotland, United Kingdom), Igor Tičar, Ph.D (Rector of the University of Maribor, Slovenia), Niko Samec Ph.D. (Pro-rector of University of Maribor, Slovenia), Zdravko Kravanja, Ph-D. (Dean of the Faculty of Chemistry and Chemical Engineering, University of Maribor, Slovenia).
- Organising Committee:** Jurij Kroppe, Ph.D. (University of Maribor, Slovenia), Darko Goričanec, Ph.D. (University of Maribor, Slovenia), Stane Božičnik, Ph.D. (University of Maribor, Slovenia), Peter Trop, Ph.D. (University of Maribor, Slovenia), Danijela Urbanč, Ph.D. (University of Maribor, Slovenia), Sonja Roj (University of Maribor, Slovenia), Željko Knez, Ph.D. (University of Maribor, Slovenia), Bojan Štumberger, Ph.D. (University of Maribor, Slovenia), Franci Čuš, Ph.D. (University of Maribor, Slovenia), Miloš Bogataj, Ph.D. (University of Maribor, Slovenia), Janez Žlak, Ph.D (Mine Trbovlje Hrustnik, Slovenia), LL. M. Tina Žagar (Ministry of Economic Development and Technology), Igor Ivanovski, MSc. (IVD Maribor, Slovenia), Nuša Hojnik, Ph.D. (Health Center Maribor).
- Programme Committee:** Prof. Abdul Ghani Olabi (UK), Emeritus Prof. Jurij Kroppe (Slovenia), Prof. Henrik Lund (Denmark), Prof. Brian Norton (Ireland), Prof. Noam Lior (USA), Prof. Zdravko Kravanja (Slovenia), Prof. Jiri Jaromír Klemesš (Hungary), Prof. Stane Božičnik (Slovenia), Prof. Bojan Štumberger (Slovenia), Prof. Soteris Kalogirou (Cyprus), Prof. Stefano Cordiner (Italy), Prof. Jinyue Yan (Sweden), Prof. Umberto Desideri (Italy), Prof. M.S.J. Hashmi (Ireland), Prof. Michele Dassisti (Italy), Prof. Michele Gambino (Italy), Prof. S. Orhan Akansu (Turkey), Dr. David Timoney (Ireland), Prof. David Kennedy (Ireland), Prof. Bekir Sami Yilbas (Saudi Arabia), Dr. Brid Quilty (Ireland), Prof. B. AbuHijleh (UAE), Prof. Vincenc Butala (Slovenia), Prof. Jim McGovern (Ireland), Prof. Socrates Kaplanis (Greece), Dr. Hussam Jouhara (UK), Prof. Igor Tičar (Slovenia), Prof. Darko Goričanec (Slovenia), Dr. Joseph Stokes (Ireland), Prof. Antonio Valero (Spain), Prof. Aristide F. Massardo (Italy), Prof. Ashwani Gupta (USA), Dr. Aoife Foley (UK), Dr. Athanasios Megartīs (UK), Prof. Francesco Di Maria (Italy), Prof. George Tsatsaronis (Germany), Prof. Luis M. Serra (Spain), Prof. Savvas Tassou (UK), Prof. Luigi Alloca (Italy), Prof. Faek Diko (Germany), Dr. F. Al-Mansour (Slovenia), Dr. Artur Grunwald (Germany), Dr. Peter Trop (Slovenia), Prof. Philippe Knauth (France), Prof. Paul Borza (Romania), Prof. Roy Douglas (UK), Prof. Dieter Meissner (Austria), Dr. Danijela Urbanč (Slovenia), Prof. Daniel Favrat (Switzerland), Prof. Erik Dahlquist (Sweden), Prof. Eric Leonhardt (USA), Prof. GianLuca Rospi (Italy), Prof. Giuseppe Casalino (Italy), Prof. J. Dawson (USA), Dr. José Simoes (Portugal), Prof. Kadir Aydin (Turkey), Dr. Khaled Benyounis (Ireland), Prof. Laszlo Garbai (Hungary), Prof. Mariano Martin (Spain), Prof. Masahiro Ishida (Japan), Prof. Michael Seal (USA), Prof. Marco Spinedi (Italy), Prof. Michio Kitano (Japan), Prof. Milovan Jotanović (BiH), Prof. Nafiz Kahraman (Turkey), Prof. Na Zhang (China), Prof. Naotake Fujita (Japan), Prof. Niko Samec (Slovenia), Prof. Oleksandr Zaporozhets (Ukraine), Prof. Osama Al-Hawaj (Kuwait), Prof. Petar Varbanov (Hungary), Prof. Peter Goethals (Belgium), Prof. Qi Zhang (China), Prof. Rik Baert (The Netherlands), Prof. Rolf Ritz (USA), Dr. Stephen Glover (UK), Prof. Signe Kjelstrup (Norway), Dr. Sumsun Naheer (UK), Prof. Sven Andersson (Sweden), Dr. Salah Ibrahim (UK), Prof. Sebahattin Unalan (Turkey), Prof. Sabah Abdul-Wahab Sulaiman (Oman), Prof. Somrat Kerdsuwan (Thailand), Prof. T. Hikmet Karakoç (Turkey), Prof. Tahir Yavuz (Turkey), Prof. Hon Loong Lam (Thailand), LL.M. Tina Žagar (Slovenia), Prof. A.M.Hamoda (Qatar), Prof. Gu Hongchen (China), Prof. Haşmet Turkoglu (Turkey), Dr. Hussam Achour (Ireland), Dr. James Carton (Ireland), Dr. Eivind Johannes (Norway), Prof. Elvis Ahmetović (BiH), Prof.

D.G.Simeonov (Bulgaria), Prof. Abdelakder Outzourhit (Morocco), Prof. Bilge Albayrak Çeçer (Turkey), Prof. Bekir Zühtü Uysal (Turkey), Prof. D. Bradley (UK), Dr. Silvia Tedesco (UK), Dr. Valentin Ivanov (Germany), Dr. Vincent Lawlor (Austria), Prof. Yonghua Cheng (Belgium), Prof. Yasufumi Yoshimoto (Japan), Prof. Yahya Erkan Akansu (Turkey), Prof. Yunus Ali Çengel (Turkey), Prof. Zeljko Knez (Slovenia), Prof. Zoltan Magyar (Hungary), Dr. William Smith (Ireland), Dr. Abed Alaswad (UK).

**First published** in 2017 by  
University of Maribor Press  
Slomškovo trg 15, 2000 Maribor, Slovenia  
tel. +386 2 250 42 42, fax +386 2 252 32 45  
<http://press.um.si>, [zalozba@um.si](mailto:zalozba@um.si)

**Co-published by**  
University of Maribor, Faculty of Chemistry and Chemical Engineering  
Smetanova ulica 17, 2000 Maribor, Slovenia  
tel. +386 (0)2 22 94 400, faks + 386 (0)2 25 27 774  
<http://www.fkkt.um.si>, [fkkt@um.si](mailto:fkkt@um.si)

**Published:** 5. July 2017

**© University of Maribor Press**

All rights reserved. No part of this book may be reprinted or reproduced or utilized in any form or by any electronic, mechanical, or other means, now known or hereafter invented, including photocopying and recording, or in any information storage or retrieval system, without permission in writing from the publisher.

CIP - Kataložni zapis o publikaciji  
Univerzitetna knjižnica Maribor

620.92/.98:502.131.1(082) (0.034.2)

INTERNATIONAL Conference on Sustainable Energy and Environmental Protection (10 ; 2017 ; Bled)

Combined and hybrid energy systems [Elektronski vir] : (Conference proceedings) / 10th International Conference on Sustainable Energy and Environmental Protection, (June 27th-30th, 2017, Bled, Slovenia) ; [organised by] University of Maribor [and] University of the West of Scotland ; editors Jurij Krope ... [et al.]. - El. zbornik. - Maribor : University of Maribor Press, 2017

Način dostopa (URL): <http://press.um.si/index.php/ump/catalog/book/240>

ISBN 978-961-286-049-3 (pdf)

doi: 10.18690/978-961-286-049-3

1. Gl. stv. nasl. 2. Krope, Jurij 3. Univerza (Maribor)

COBISS.SI-ID [92422145](https://nbn-resolving.org/urn:nbn:si:coibis-92422145)

**ISBN** 978-961-286-049-3

**DOI:** <https://doi.org/10.18690/978-961-286-049-3>

**Price:** Free copy

**For publisher:** Prof. Igor Tičar, Ph.D., rector (University of Maribor)

## Preface

The 10<sup>th</sup> International Conference on Sustainable Energy and environmental Protection – SEEP 2017 was organised on June 27<sup>th</sup> – 30<sup>th</sup> 2017 in Bled, Slovenia, by:

- Faculty of Chemistry and Chemical Engineering, University of Maribor, Slovenia,
- University of the West of Scotland, School of Engineering and

The aim of SEEP2017 is to bring together the researches within the field of sustainable energy and environmental protection from all over the world.

The contributed papers are grouped in 18 sessions in order to provide access to readers out of 300 contributions prepared by authors from 52 countries.

We thank the distinguished plenary and keynote speakers and chairs who have kindly consented to participate at this conference. We are also grateful to all the authors for their papers and to all committee members.

We believe that scientific results and professional debates shall not only be an incentive for development, but also for making new friendships and possible future scientific development projects.

General chair  
Emeritus Prof. dr. Jurij Krope



## Plenary Talk on The Relation between Renewable Energy and Circular Economy

ABDUL GHANI OLABI- BIBLIOGRAPHY



Prof Olabi is director and founding member of the Institute of Engineering and Energy Technologies ([www.uws.ac.uk/ieet](http://www.uws.ac.uk/ieet)) at the University of the West of Scotland. He received his M.Eng and Ph.D. from Dublin City University, since 1984 he worked at SSRC, HIAST, CNR, CRF, DCU and UWS. Prof Olabi has supervised postgraduate research students (10 M.Eng and 30PhD) to successful completion. Prof Olabi has edited 12 proceedings, and has published more than 135 papers in peer-reviewed international journals and about 135 papers in international conferences, in addition to 30 book chapters. In the last 12 months Prof Olabi has patented 2 innovative projects. Prof Olabi is the founder of the International Conference on Sustainable Energy and Environmental Protection SEEP, [www.seepconference.co.uk](http://www.seepconference.co.uk)

He is the Subject Editor of the Elsevier Energy Journal <https://www.journals.elsevier.com/energy/editorial-board/abdul-ghani-olabi>, also Subject editor of the Reference Module in Materials Science and Materials Engineering <http://scitechconnect.elsevier.com/reference-module-material-science/> and board member of a few other journals. Prof Olabi has coordinated different National, EU and International Projects. He has produced different reports to the Irish Gov. regarding: Hydrogen and Fuel Cells and Solar Energy.

---

CORRESPONDENCE ADDRESS: Abdul Ghani Olabi, Ph.D., Professor, University of the West of Scotland, School of Engineering and Computing, D163a, McLachlan Building, Paisley, United Kingdom, e-mail: [Abdul.Olabi@uws.ac.uk](mailto:Abdul.Olabi@uws.ac.uk).

<https://doi.org/10.18690/978-961-286-049-3> ISBN 978-961-286-049-3  
© 2017 University of Maribor Press  
Available at: <http://press.um.si>.

## **Plenary Talk on Energy Footprints Reduction and Virtual Footprints Interactions**

JIRÍ JAROMÍR KLEMEŠ & PETAR SABEV VARBANOV

Increasing efforts and resources have been devoted to research during environmental studies, including the assessment of various harmful impacts from industrial, civic, business, transportation and other economy activities. Environmental impacts are usually quantified through Life Cycle Assessment (LCA). In recent years, footprints have emerged as efficient and useful indicators to use within LCA. The footprint assessment techniques has provided a set of tools enabling the evaluation of Greenhouse Gas (GHG) – including CO<sub>2</sub>, emissions and the corresponding effective flows on the world scale. From all such indicators, the energy footprint represents the area of forest that would be required to absorb the GHG emissions resulting from the energy consumption required for a certain activity, excluding the proportion absorbed by the oceans, and the area occupied by hydroelectric dams and reservoirs for hydropower.

An overview of the virtual GHG flow trends in the international trade, associating the GHG and water footprints with the consumption of goods and services is performed. Several important indications have been obtained: (a) There are significant GHG gaps between producer's and consumer's emissions – US and EU have high absolute net imports GHG budget. (b) China is an exporting country and increasingly carries a load of GHG emission and virtual water export associated with consumption in the relevant importing countries. (c) International trade can reduce global environmental pressure by redirecting import to products produced with lower intensity of GHG emissions and lower water footprints, or producing them domestically.

To develop self-sufficient regions based on more efficient processes by combining neighbouring countries can be a promising development. A future direction should be focused on two main areas: (1) To provide the self-sufficient regions based on more efficient processes by combining production of surrounding countries. (2) To develop the shared mechanism and market share of virtual carbon between trading partners regionally and internationally.

---

CORRESPONDENCE ADDRESS: Jiří Jaromír Klemeš, DSc, Professor, Brno University of Technology - VUT Brno, Faculty of Mechanical Engineering, NETME Centre, Sustainable Process Integration Laboratory – SPIL, Technická 2896/2, 616 69 Brno, Czech Republic, e-mail: klemes@fme.vutbr.cz. Petar Sabev Varbanov, Ph.D., Associate Professor, Brno University of Technology - VUT Brno, Faculty of Mechanical Engineering, NETME Centre, Sustainable Process Integration Laboratory – SPIL, Technická 2896/2, 616 69 Brno, Czech Republic, e-mail: varbanov@fme.vutbr.cz.

## JIŘÍ JAROMÍR KLEMEŠ - BIBLIOGRAPHY



Head of “Sustainable Process Integration Laboratory – SPIL”, NETME Centre, Faculty of Mechanical Engineering, Brno University of Technology - VUT Brno, Czech Republic and Emeritus Professor at “Centre for Process Systems Engineering and Sustainability”, Pázmány Péter Catholic University, Budapest, Hungary.

Previously the Project Director, Senior Project Officer and Hon Reader at Department of Process Integration at UMIST, The University of Manchester and University of Edinburgh, UK. Founder and a long term Head of the Centre for Process Integration and Intensification – CPI2, University of Pannonia, Veszprém, Hungary. Awarded by the EC with Marie Curies Chair of Excellence (EXC). Track record of managing and coordinating 91 major EC, NATO and UK Know-How projects. Research funding attracted over 21 M€.

Co-Editor-in-Chief of Journal of Cleaner Production (IF=4.959). The founder and President for 20 y of PRES (Process Integration for Energy Saving and Pollution Reduction) conferences. Chairperson of CAPE Working Party of EFCE, a member of WP on Process Intensification and of the EFCE Sustainability platform.

He authored nearly 400 papers, h-index 40. A number of books published by McGraw-Hill; Woodhead; Elsevier; Ashgate Publishing Cambridge; Springer; WILEY-VCH; Taylor & Francis).

Several times Distinguished Visiting Professor for Universiti Teknologi Malaysia, Xi’an Jiaotong University; South China University of Technology, Guangzhou; Tianjin University in China; University of Maribor, Slovenia; University Technology Petronas, Malaysia; Brno University of Technology and the Russian Mendeleev University of Chemical Technology, Moscow. Doctor Honoris Causa of Kharkiv National University “Kharkiv Polytechnic Institute” in Ukraine, the University of Maribor in Slovenia, University POLITEHNICA Bucharest, Romania. “Honorary Doctor of Engineering Universiti Teknologi Malaysia”, “Honorary Membership of Czech Society of Chemical Engineering”, “European Federation of Chemical Engineering (EFCE) Life-Time Achievements Award” and “Pro Universitaire Pannonica” Gold Medal

---

CORRESPONDENCE ADDRESS: Jiří Jaromír Klemeš, DSc, Professor, Brno University of Technology - VUT Brno, Faculty of Mechanical Engineering, NETME Centre, Sustainable Process Integration Laboratory – SPIL, Technická 2896/2, 616 69 Brno, Czech Republic, e-mail: klemes@fme.vutbr.cz.

## **Plenary Talk on Renewable energy sources for environmental protection**

HAKAN SERHAD SOYHAN

Development in energy sector, technological advancements, production and consumption amounts in the countries and environmental awareness give shape to industry of energy. When the dependency is taken into account in terms of natural resources and energy, there are many risks for countries having no fossil energy sources. Renewable and clean sources of energy and optimal use of these resources minimize environmental impacts, produce minimum secondary wastes and are sustainable based on current and future economic and social societal needs. Sun is one of the main energy sources in recent years. Light and heat of sun are used in many ways to renewable energy. Other commonly used are biomass and wind energy. To be able to use these sources efficiently national energy and natural resources policies should be evaluated together with the global developments and they should be compatible with technological improvements. Strategic plans with regard to energy are needed more intensively and they must be in the qualification of a road map, taking into account the developments related to natural resources and energy, its specific needs and defining the sources owned by countries. In this presentation, the role of supply security was evaluated in term of energy policies. In this talk, new technologies in renewable energy production will be shown and the importance of supply security in strategic energy plan will be explained

---

CORRESPONDENCE ADDRESS: Hakan Serhad Soyhan, Ph.D., Professor, Sakarya University, Engineering Faculty, Esentepe Campus, M7 Building, 54187 - Esentepe /Sakarya, Turkey, e-mail: hsoyhan@sakarya.edu.tr.

<https://doi.org/10.18690/978-961-286-049-3> ISBN 978-961-286-049-3  
© 2017 University of Maribor Press  
Available at: <http://press.um.si>.

### HAKAN SERHAD SOYHAN- BIBLIOGRAPHY



Professor at Sakarya University, Engineering Faculty. 50 % for teaching and the rest for research activities.

Teaching, courses taught:

Graduate courses:

- Combustion technology;
- Modelling techniques;

Undergraduate courses:

- Combustion techniques;
- Internal combustion engines;
- Fire safety.

Technical skills and competences professional societies:

- 25 journal papers in SCI Index. 23 conference papers;
- Editor at FCE journal. Co-editor at J of Sakarya University;
- Head of Local Energy Research Society (YETA);
- Member of American Society of Mechanical Engineers (ASME);
- Member of Turkish Society of Mechanical Engineers (TSME).

---

CORRESPONDENCE ADDRESS: Hakan Serhad Soyhan, Ph.D., Professor, Sakarya University, Engineering Faculty, Esentepe Campus, M7 Building, 54187 - Esentepe /Sakarya, Turkey, e-mail: hsoyhan@sakarya.edu.tr.



## Table of Contents

### CONFERENCE PROCEEDINGS

<b>Penetration of Renewable Sources in Microgrids: Effects of MILP – Based Control Strategies</b>	<b>1</b>
Bartolucci Lorenzo, Cordiner Stefano, Mulone Vincenzo, Rocco Vittorio & Rossi Joao Luis	
<b>Hybrid Renewable Systems for Microgrids: Influence of System Sizing on Performances</b>	<b>17</b>
Bartolucci Lorenzo, Cordiner Stefano, Mulone Vincenzo, Rocco Vittorio & Rossi Joao Luis	
<b>Triple Domestic Heat Recovery System: Thermal Modeling and Parametric Study</b>	<b>33</b>
Hassan Jaber, Mahmoud Khaled, Thierry Lemenand, Rabih Murr, Jalal Faraja & Mohamad Ramadana	
<b>A Wind Park – Pumped Hydro Storage Plant Towards 100% Energy Autonomy for The Island of Sifnos, Greece. Perspectives Created from Energy Cooperatives</b>	<b>49</b>
Dimitris Al. Katsaprakakis	
<b>Effect of Fuel Composition Fluctuation on the Safety Performance of an it-SOFC/GT Hybrid System</b>	<b>61</b>
Zhe Chen, Feng Tian, Xiaojing Lv, Xiaoyi Ding & Yiwu Weng	



## Penetration of Renewable Sources in Microgrids: Effects of MILP – Based Control Strategies

BARTOLUCCI LORENZO, CORDINER STEFANO, MULONE VINCENZO, ROCCO VITTORIO & ROSSI JOAO LUIS

**Abstract** The rapid growth of the Distributed Generation (DG) concept has given technical issues regarding the integration and control within the grid nodes. A predictive control strategy integrating renewable and non-renewable sources as well as energy storage within the grid, is a potential solution to face with the mentioned issues. The behavior of a smart building of 30 apartments has been considered in this work. The Hybrid Renewable System has been controlled by a Model Predictive Control (MPC) strategy. The HRS includes sub-systems for the conversion of renewable energy sources as well as non-renewable ones connected to the main grid. Several scenarios have been tested under different weather conditions and in terms of renewable sources penetration. Results obtained with the MPC control strategy have been compared with a Rule Based Control (RBC). Results show that the use of MPC improves the integration of the residential microgrid with the renewable sources connected to the grid thanks to the predictive system smoothing out the energy demand profile and absorbing the peak production from the photovoltaic and wind farms, even in the cases of higher penetration.

**Keywords:** • DC MicroGrids • Model predictive control • Fuel cells • Distributed generation • Renewable energy source • Demand Response •

---

CORRESPONDENCE ADDRESS: Bartolucci Lorenzo, Ph.D., University of Rome Tor Vergata, Department of Industrial Engineering, via del Politecnico 1, 00133 Rome, Italy, e-mail: [lorenzo.bartolucci@uniroma2.it](mailto:lorenzo.bartolucci@uniroma2.it). Cordiner Stefano, Ph.D., Full Professor, University of Rome Tor Vergata, Department of Industrial Engineering, via del Politecnico 1, 00133 Rome, Italy, e-mail: [cordiner@uniroma2.it](mailto:cordiner@uniroma2.it). Mulone Vincenzo, Ph.D., Associate Professor, University of Rome Tor Vergata, Department of Industrial Engineering, via del Politecnico 1, 00133 Rome, Italy, e-mail: [mulone@uniroma2.it](mailto:mulone@uniroma2.it). Rocco Vittorio, Ph.D., Full Professor, University of Rome Tor Vergata, Department of Industrial Engineering, via del Politecnico 1, 00133 Rome, Italy, e-mail: [rocco@uniroma2.it](mailto:rocco@uniroma2.it). Rossi Joao Luis, Ph.D., University of Rome Tor Vergata, Department of Industrial Engineering, via del Politecnico 1, 00133 Rome, Italy, e-mail: [joao.luis.rossi@uniroma2.it](mailto:joao.luis.rossi@uniroma2.it).

## 1 Introduction

Fostered by environmental concerns, technological evolution and economic improvements, distributed energy resources (DERs) are expected to play a major role in the future of electrical power delivery [1].

Despite the growth and the benefits of renewable systems, there are uncertainties regarding the stability of the grid connected to intermittent, floating, unpredictable and non-programmable sources of energy, especially referring to mini and micro-producers of energy interfacing with the grid. Moreover, the energy produced from the non-programmable RES, normally, does not match with the local demand, limiting the overall penetration in the system.

In such a context, control and scheduling strategies, mainly at the residential level, are becoming a key aspect for improving the system stability overall, and maximizing RES exploitation. Energy Storage System (ESS) [2, 3] seem a good solution to handle power peaks and fluctuations. Energy can be stored by means of different technologies, such as pumping hydroelectric systems [4], hydrogen technologies (electrolyzes towards gas storage systems) [5] or power to gas concepts [6], that unfortunately, have technical and economical flaws. Electrical storage systems are a feasible techno-economic solution [7] with excellent performance in terms of renewable energy integration [8, 9], as shown in a new project, led by Terna, for their integration into the Italian main electric grid [10]. Moreover, load shifting, Demand Side Management strategies (DSM) [11] and Demand Response policies (DR) have demonstrated good results to compensate for renewable sources fluctuations increasing their penetration [12]. In this paper two control strategies have been considered to analyze the mentioned effects of RES penetration into a microgrid system: a RBC control strategy, and an optimized one based on MPC. A case study of 30 residential apartments has been investigated at different levels of RES penetration. Both energy-based and economic aspects have been taken into account in the analysis of the results to compare the performance of the MPC strategy with the RBC one.

## 2 Residential Microgrid

The design of Microgrid power systems is a crucial and complex aspect that is highly affected by local weather [13, 14]. Thus, Homer® software was used to guess the sizing of each subsystem within the Microgrid.

The MicroGrid layout here considered is based on a battery bank is connected directly to the DC Bus, which in turn controls the system voltage. The residential load and the power grid are connected to the DC Bus through an AC/DC converter and the FC and PV are connected to the DC bus through DC/DC converters. More details are given below (Figure 1).

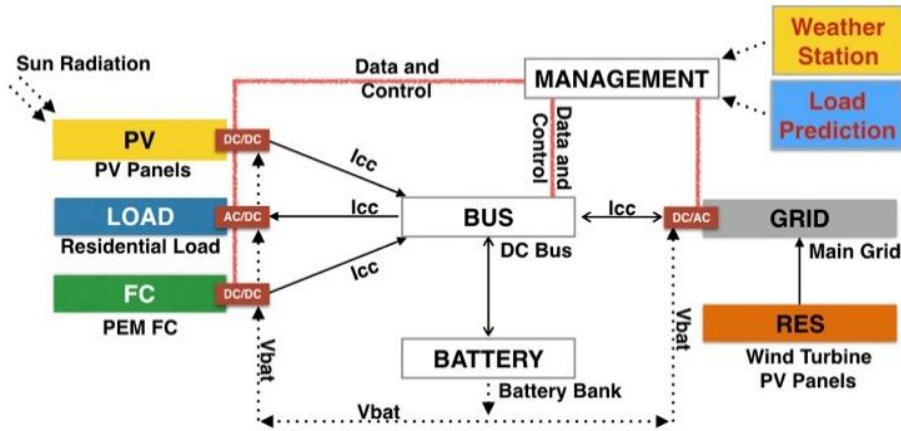


Figure 1 – Schematics of the microgrid

The definition of the residential load is crucial, depending on appliance technology and individual scheduling strategies [15-17], as well as on social factors, household occupation, regional culture, lifestyle, etc. [18].

Therefore, special attention was given to the definition of residential load, through the use of probabilistic data, in relation to the most common household appliances found, the probability of use and usual hours in the areas around Rome – Italy, considering lighting, electric boiler, electric oven, refrigerator, microwave oven, PC, TV-set, dishwasher, washing machine and dryer.

### 3 Control Models

#### 3.1 Rule-based management system (RBC)

The RBC strategies have been extensively investigated when dealing with microgrid power management for their simplicity and robustness [19], consisting in rules based on threshold values and pre-established operating constraints [20]. A voltage based model was implemented and validated against experimental data. The Rules used in the control model are same as [21], where more details are available.

#### 3.2 Model predictive control (MPC)

The MPC strategies with MILP formulation have been tested, obtaining outstanding performances, in experimental microgrids in Athens [22] or in the Savona campus [23].

The results have shown a good performance and computational processing capacity of the proposed algorithm, and there is still room for improvement.

A model MPC problem can be synthesized in the form:

$$\begin{aligned} x_{k+1} &= A \cdot x_k + B \cdot u_k + B_d \cdot d_k + B_w \cdot w_k \\ y_k &= C \cdot x_k \end{aligned} \quad (1)$$

Where:  $y_k$  represents the output of the system,  $x_k$  is the state,  $u_k$  is the control variable,  $d_k$  is an external disturbance and  $w_k$  is the uncertainty in the system.

The Fuel Cell has been modeled by means of following variables:

$$P_{FC}, \delta_{on/off}, \delta_{standby}, \delta_{start\ up}$$

The first is a continuous variable that represents the fuel cell output power; second, third and fourth are binary variables representing FC on/off status, FC stand-by operation mode, FC start up. For these variables, following constraints have been considered the limits:

$$P_{FC|t} - P_{FC|P} x \delta_{on/off|t} \leq 0 \quad (2)$$

$$-P_{FC|t} + P_{FC|stby} x \delta_{on/off|t} \leq 0 \quad (3)$$

$$\delta_{on/off|t} + \delta_{stby|t} \leq 1 \quad (4)$$

$$\delta_{on/off|t} + \delta_{stby|t} - \delta_{startup|t} - \delta_{on/off|t-1} + \delta_{stby|t-1} \leq 1 \quad (5)$$

The first and second constraints limits the power produced by the FC within  $P_{FC|P}$  and  $P_{FC|stby}$ , when  $\delta_{(on/off|t)}$  is equal to 1 (operative mode), third equation avoid simultaneous operation of standby or operative modes. The last equation quantifies the number of FC start-ups. Subscript ( $t$ ) is used to refer to current sample time, ( $t-1$ ) instead is related to the previous sample time.

The Grid has been modeled as shown below:

$$\delta_{fromgrid}, P_{fromgrid}, \delta_{togroup}, P_{togroup}, P_{unb^+}, P_{unb^-} \quad (6)$$

The  $\delta_{fromgrid}$ ,  $\delta_{togroup}$  are binary variable representing power exchange direction respect to the main grid. To limit the maximum power up in both directions and to avoid simultaneous positive and e negative power flow, the following constrains have been defined:

$$P_{fromgrid|t} - P_{fromgrid|P} x \delta_{fromgrid|t} \leq 0 \quad (7)$$

$$P_{togroup|t} - P_{togroup|P} x \delta_{togroup|t} \leq 0 \quad (8)$$

$$\delta_{togrid|t} + \delta_{fromgrid|t} \leq 1 \quad (9)$$

$$P_{fromgrid|t}, P_{togrid|t}, P_{umb^+|t}, P_{umb^-|t} \geq 0 \quad (10)$$

$$P_{fromgrid|t} - P_{togrid|t} + P_{umb^+|t} - P_{umb^-|t} = P_{gridref|t} \quad (11)$$

The last equation defines the grid exchange power profile as equal to the reference; in case it cannot be maintained, power in excess ( $P_{umb^+|t}$ ,  $P_{umb^-|t}$ ) is needed to hold the equivalence. These variables will be use as soft constraints [23].

As already described before, the residence complex under study has a randomly generated load profile, following the probability of daily use for each individual household appliance.

For the management system based on the MPC/MILP algorithm, the appliances that represent the largest consumption in an Italian residence (Wash-Machine, Dryer and Dishwasher) have been controlled directly by the MPC algorithm; their activation has been controlled depending on the optimization of the algorithm.

Each appliance has been modeled by means of a binary variable for each discretized sample plus a binary variable to represent the appliances start-up. If  $p$  is the number of discrete samples used to represent the appliances profile, then a vector of  $p+1$  binary variables is developed to model the appliance. So, for each deferrable appliance, the following vector of variables is used:

$$[v_l, v_{l+1}, \dots, v_n, b] \quad (12)$$

where  $n$  is the number of sample times used to represent the appliance consumption profile.

The appliances controlled by the MPC, are subject to the following restrictions:

1. The Appliance is activated only once a day (if used in that day);
2. Following a logical condition, the Dryer can only be activated after the wash cycle ended;
3. The number of weekly uses of an appliance is strictly the probability of the amount of use described in [24];
4. After an appliance is activated by the algorithm, the cycle cannot be interrupted;

$$P_{Discretized\ power\ profile}, \quad \delta_{schedule}, \quad P_{used}$$

The  $\delta_{schedule}$  determines the most probable instant in the timeline where the appliance can be turned on, and  $\delta_{used}$  determines on the other hand if the appliance has already been turned on in the given time horizon.

$$\delta_{schedule} = 1 \text{ and } \delta_{used} = 0, t \text{ to } t+P \quad (13)$$

$$\delta_{schedule} = 0 \text{ and } \delta_{used} = 1, t+P \text{ to } t+N \quad (14)$$

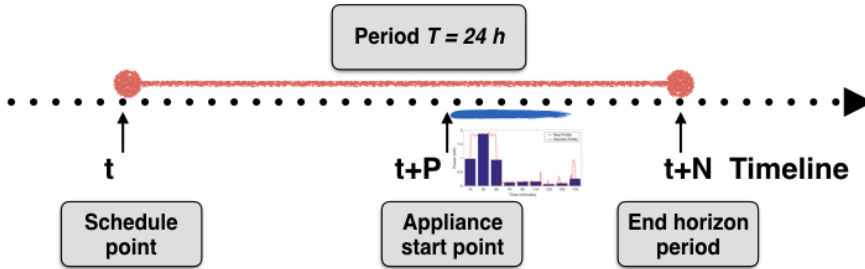


Figure 2 - Load Prediction timeline

### 3.2.1 Forecasts

The sun radiation forecast for Rome/Italy, related to the period of simulation, has been implemented into the MPC algorithm via data provided by CNMCA (Italian Air Force Meteorological Service) [25] and the real weather data, has been measured at the weather station of the University of Rome “Tor Vergata”.

Due to the lack of real historical data for residential applications, the daily simulations of the load profile of a model house have been defined with a random simulator for a period of 4 years, subtracting from the profile generated, the curves of the house appliances controlled by the MPC algorithm.

The procedure adopted to determine the errors is based on a simple linear regression of the two-data series, composed of the meteorological forecasts error at time  $k$  and at time,  $k + 1$ , as suggested in [26].

## 4 Analysis of results

A case study of 30 residential apartments was investigated for three different level of RES penetration. Two different months were tested, in particular, January and June with both the RBC and MPC control strategies.

The RES penetration was changed varying the number of wind turbines and PV panel. The details of the three simulated cases are reported in Table 1.

Table 1 – Details of the simulated cases

RES Penetration	N wind turbines	PV surface [mm <sup>2</sup> ]	% wind turbines	% PV
Minimum – sim1	7	70	5.7	7
Medium – sim2	10	100	8	10
Maximum – sim3	15	150	14.7	12

Results for 1 week of each simulated case are reported in the following to show the load and production profile. In green is reported the power produced by PV, in red by the wind turbines while in blue the energy withdrawn by the grid. The solid black line shows instead the demand profile. It is worth to notice that the energy stored in the battery is not considered in the demand profile.

In general, numerical simulations highlighted a more smoothed load profile for the MPC control strategy related to the capability of the strategy to shift the load avoid high pick temporally concentrated demand.

Moreover, Figure 3 shows how already for the lowest level of RES penetration in January the RBC control model did not allow to completely use all the energy produced by the RES.

On contrary, the MILP control strategy, moving the load where higher RES availability was present allowed for a better exploitation of the overall energy produced by the non-programmable renewable sources (Figure 4)

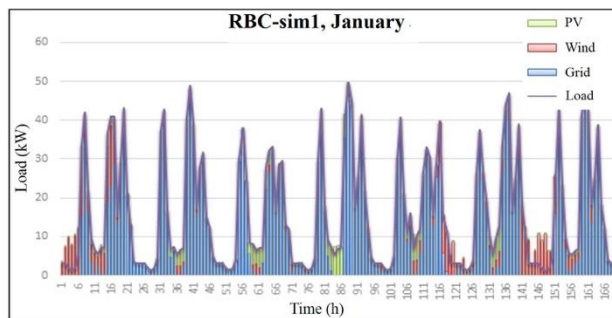


Figure 3 – Simulation for the RBC-sim1 January

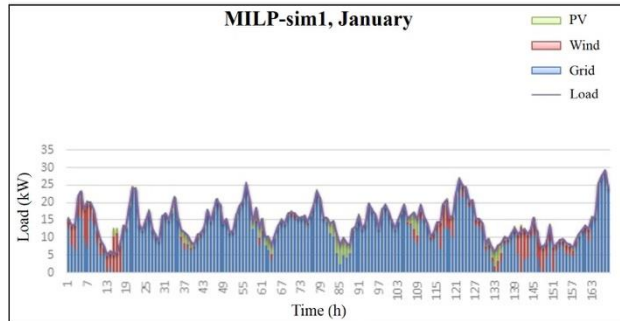


Figure 4 – Simulation for the MILP-sim1 January

Similar considerations can be drawn looking at the lower RES penetration cases for month of June. The MILP control strategy allowed for a better distribution of the energy demand covering almost all the energy produced by RES while the RBC, not having load scheduling, was not able to cover (Figures 5 - 6).

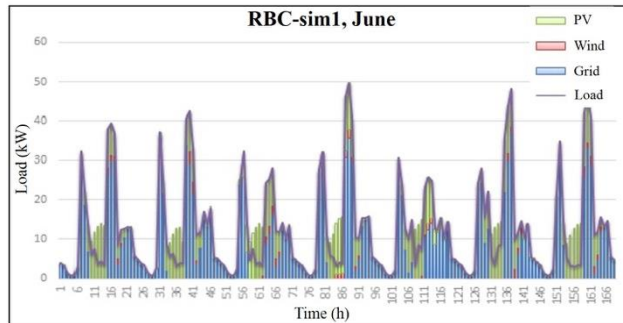


Figure 5 – Simulation for the RBC-sim1 June

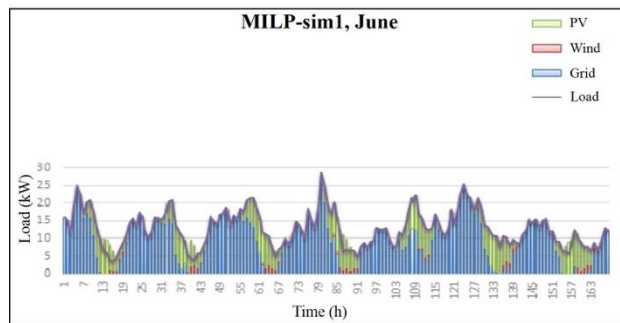


Figure 6 – Simulation for the MILP-sim1 June

B. Lorenzo, C. Stefano, M. Vincenzo, R. Vittorio & R. Joao Luis: Penetration of Renewable Sources in Microgrids: Effects of MILP – Based Control Strategies

Going towards higher RES penetration (Figures 7 – 10) the beneficial effects produced by the MPC control strategy are highlighted, the excess energy produced by RES increased for the RBC cases while the case controlled by means of a MILP based control strategy was able to move the load to reduce those excesses.

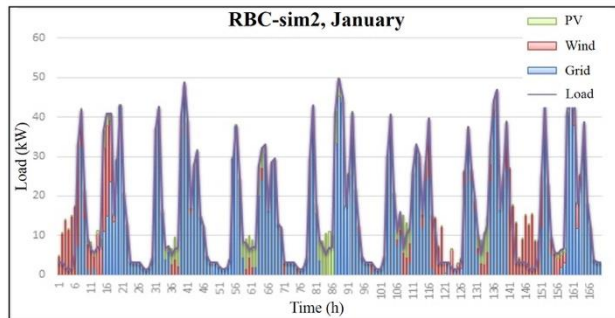


Figure 7 – Simulation for the RBC-sim2 January

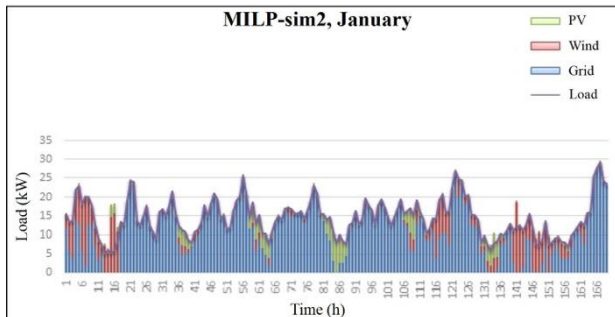


Figure 8 – Simulation for the MILP-sim2 January

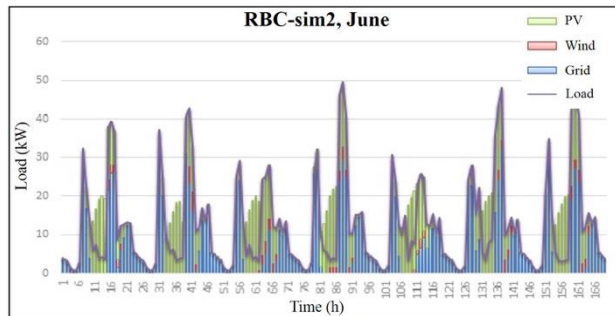


Figure 9 – Simulation for the RBC-sim2 June

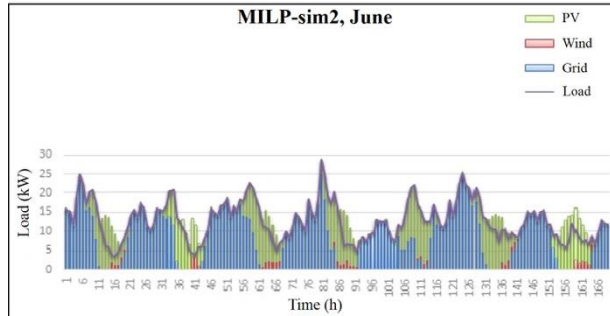


Figure 10 – Simulation for the MILP-sim2 June

Coming to the highest RES penetration (Figures 11 – 14) more evident energy excess from RES are present in the simulations. The deferrable loads were not sufficient to absorb the non-programmable renewable energy production resulting in some excesses for both strategies. This is due to the high impact of such level of RES penetration on the residential case studied. Extending the control strategy to a higher number of apartments would help to mitigate these effects.

Even for winter (January), where RES production is reduced, the MILP has shown a better performance when compared to RBC.

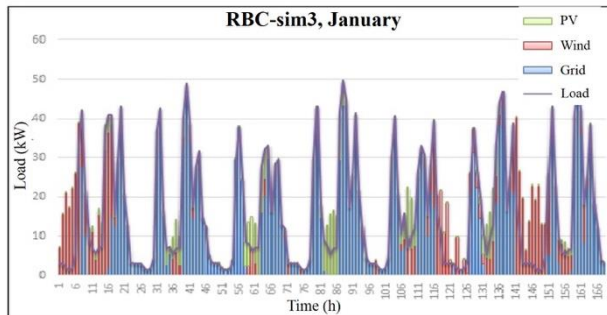


Figure 11 – Simulation for the RBC-sim3 January

B. Lorenzo, C. Stefano, M. Vincenzo, R. Vittorio & R. Joao Luis: Penetration of Renewable Sources in Microgrids: Effects of MILP – Based Control Strategies

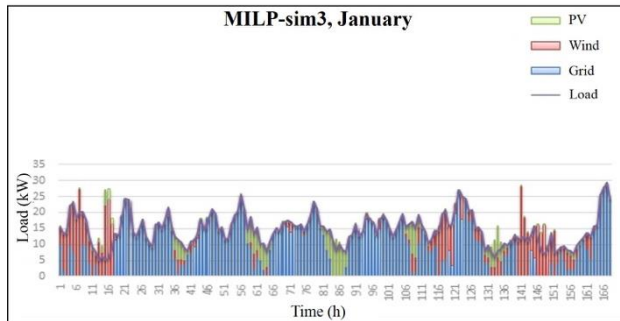


Figure 12 – Simulation for the MILP-sim3 January

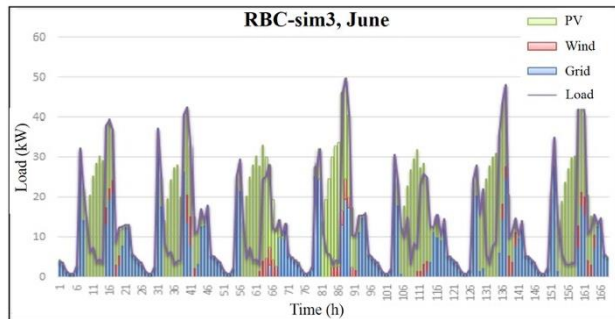


Figure 13 – Simulation for the RBC-sim3 June

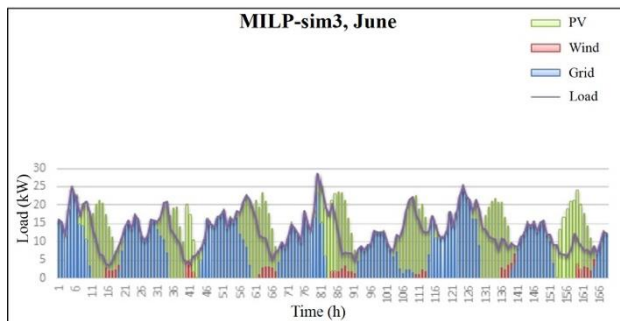


Figure 14 – Simulation for the MILP-sim3 June

In this third simulation, being summer (June), the high production from the PV exceeds the amount of energy needed to feed the load, thus, both systems have excesses. Again, due to the possibility of forecasting and scheduling of the loads, the MILP presents a better use of the renewable resources, reducing the amount of energy that is sold to the network.

## 5 Conclusions

This work presents the study of a complete Microgrid system, composed of programmable and non-programmable renewable energy sources, short and long term energy storage and the use of efficient control strategies for the management of production and consumption, until having the goal of contributing to the sustainable implementation of Smart Grid and Distributed Generation concepts.

The RBC and MPC control strategies were compared in order to analyze different technical solutions to encourage the penetration of renewables in the network.

- Performance increase strongly whenever a DSM, using predictive control logic, has been added to the system;
- The use of a battery-coupled with DMS helps reducing fluctuations in power exchanged with the grid, increasing the stability from both the end-user and the network provider side;
- Thanks to the management of the load in the MILP was possible to verify an important reduction of the peaks and linearization of the consumption from the grid.
- Due to the management of the equipment was possible to move certain loads for periods of greater production of the renewables.

The results showed that by including a DSM strategies with prediction, residential users can adapt their consumption profiles to a better interaction with the grid, and thus the residential Microgrids can act as a kind of auxiliary service, strongly favoring RES penetration in the grid.

From the economics point of view, using electricity cost in accordance with a Peak Demand Charge strategy that consists in accounting a higher cost for the higher adsorbed power, the MILP strategy offer an advantage as well. In particular, the capability of the model to linearize the exchange with the grid (Figure 15) led to a reduction of cost of about 34-36% for the months of January and June (Figure 16). Showing how the use of such control strategy represents an advantage for both the provider and the consumers.

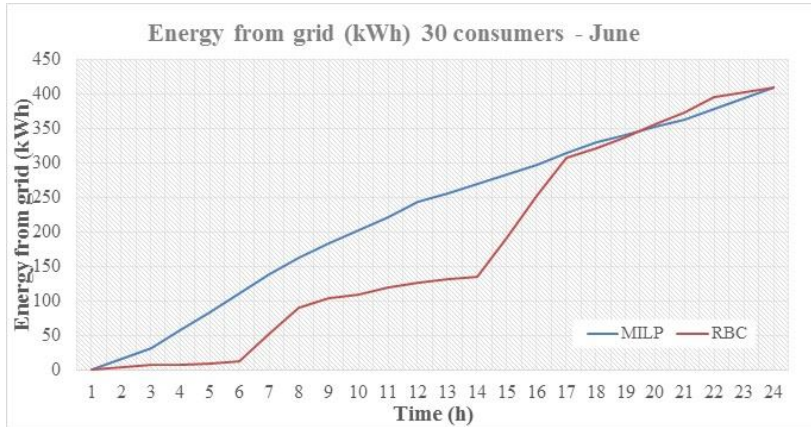


Figure 15 – Energy withdrawn from grid for 30 consumers, comparison between MILP and RBC strategies - June.

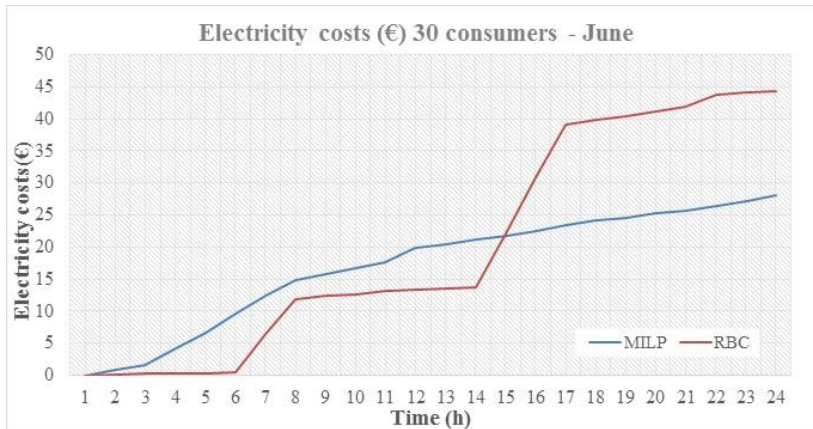


Figure 16 – Electricity costs for 30 consumers, comparison between MILP and RBC strategies - June.

### Acknowledgements

The authors would like to acknowledge the master student Andrea Rocca for his valuable contribution to the numerical results commented in this paper and CSF/CAPES (BEX-11965/13-4) – Brazilian Federal Agency for Support and Evaluation of Graduate Education within the Ministry of Education of Brazil.”

### References

- [1] REN21. (2015, 14/04/2016). *Renewables Global Status Report (GSR)*. Available:

<http://www.ren21.net/status-of-renewables/>

- [2] A. Evans, V. Strezov, and T. J. Evans, "Assessment of utility energy storage options for increased renewable energy penetration," *Renewable & Sustainable Energy Reviews*, vol. 16, no. 6, pp. 4141-4147, Aug 2012.
- [3] X. G. Tan, Q. M. Li, and H. Wang, "Advances and trends of energy storage technology in Microgrid," *International Journal of Electrical Power & Energy Systems*, vol. 44, no. 1, pp. 179-191, Jan 2013.
- [4] D. Connolly, H. Lund, B. V. Mathiesen, E. Pican, and M. Leahy, "The technical and economic implications of integrating fluctuating renewable energy using energy storage," *Renewable Energy*, vol. 43, pp. 47-60, Jul 2012.
- [5] G. Bruni *et al.*, "Fuel cell based power systems to supply power to Telecom Stations," *International Journal of Hydrogen Energy*, vol. 39, no. 36, pp. 21767-21777, Dec 2014.
- [6] G. Guandalini, S. Campanari, and M. C. Romano, "Power-to-gas plants and gas turbines for improved wind energy dispatchability: Energy and economic assessment," *Applied Energy*, vol. 147, pp. 117-130, Jun 2015.
- [7] A. A. Solomon, D. M. Kammen, and D. Callaway, "The role of large-scale energy storage design and dispatch in the power grid: A study of very high grid penetration of variable renewable resources," *Applied Energy*, vol. 134, pp. 75-89, Dec 2014.
- [8] P. A. Ostergaard, "Comparing electricity, heat and biogas storages' impacts on renewable energy integration," *Energy*, vol. 37, no. 1, pp. 255-262, Jan 2012.
- [9] B. Dunn, H. Kamath, and J. M. Tarascon, "Electrical Energy Storage for the Grid: A Battery of Choices," *Science*, vol. 334, no. 6058, pp. 928-935, Nov 2011.
- [10] F. Palone *et al.*, "Commissioning and testing of the first Lithium-Titanate BESS for the Italian Transmission Grid," *2015 Ieee 15th International Conference on Environment and Electrical Engineering (Ieee Eeeic 2015)*, pp. 1025-1030, 2015.
- [11] A. Pina, C. Silva, and P. Ferrao, "The impact of demand side management strategies in the penetration of renewable electricity," *Energy*, vol. 41, no. 1, pp. 128-137, May 2012.
- [12] B. Schafer, M. Matthiae, M. Timme, and D. Withaut, "Decentral smart grid control (vol 17, 015002, 2015)," *New Journal of Physics*, vol. 17, May 2015, Art. no. 059502.
- [13] J. Weniger, T. Tjaden, V. Quaschnig, and Eurosolar, "Sizing of residential PV battery systems," *8th International Renewable Energy Storage Conference and Exhibition (Ires 2013)*, vol. 46, pp. 78-87, 2014.
- [14] Y. S. Mohammed, M. W. Mustafa, and N. Bashir, "Hybrid renewable energy systems for off-grid electric power: Review of substantial issues," *Renewable & Sustainable Energy Reviews*, vol. 35, pp. 527-539, Jul 2014.
- [15] M. Beaudin and H. Zareipour, "Home energy management systems: A review of modelling and complexity," *Renewable & Sustainable Energy Reviews*, vol. 45, pp. 318-335, May 2015.
- [16] J. K. Gruber, S. Jahromizadeh, M. Prodanovic, and V. Rakocevic, "Application-oriented modelling of domestic energy demand," *International Journal of Electrical Power & Energy Systems*, vol. 61, pp. 656-664, Oct 2014.
- [17] D. Fischer, A. Hartl, and B. Wille-Hausmann, "Model for electric load profiles with high time resolution for German households," *Energy and Buildings*, vol. 92, pp. 170-179, Apr 2015.
- [18] Y. Riffonneau, S. Bacha, F. Barruel, and S. Ploix, "Optimal power flow management for grid connected PV systems with Batteries," *Ieee Transactions on Sustainable Energy*, vol. 2, no. 3, pp. 309-320, Jul 2011.
- [19] D. Giaouris *et al.*, "Performance investigation of a hybrid renewable power generation and storage system using systemic power management models," *Energy*, vol. 61, pp. 621-635,

B. Lorenzo, C. Stefano, M. Vincenzo, R. Vittorio & R. Joao Luis: Penetration of  
Renewable Sources in Microgrids: Effects of MILP – Based Control Strategies

Nov 2013.

- [20] G. Bruni, S. Cordiner, and V. Mulone, "Domestic distributed power generation: Effect of sizing and energy management strategy on the environmental efficiency of a photovoltaic-battery-fuel cell system," *Energy*, vol. 77, pp. 133-143, Dec 2014.
- [21] A. Parisio, E. Rikos, and L. Glielmo, "A Model Predictive Control Approach to Microgrid Operation Optimization," *Ieee Transactions on Control Systems Technology*, vol. 22, no. 5, pp. 1813-1827, Sep 2014.
- [22] S. Bracco, F. Delfino, F. Pampararo, M. Robba, and M. Rossi, "A dynamic optimization-based architecture for poly-generation microgrids with tri-generation, renewables, storage systems and electrical vehicles," *Energy Conversion and Management*, vol. 96, pp. 511-520, May 2015.
- [23] F. Oldewurtel, C. N. Jones, A. Parisio, and M. Morari, "Stochastic Model Predictive Control for Building Climate Control," *Ieee Transactions on Control Systems Technology*, vol. 22, no. 3, pp. 1198-1205, May 2014.
- [24] E. R. G.-. eERG. (2010). *Measurements of electrical energy consumption in the domestic sector* *Measurements of electrical energy consumption in the domestic sector*.
- [25] CNMCA. (2017). *Homepage | MeteoAM.it - Air Force Weather Service*. Available: <http://www.meteoam.it/>
- [26] G. Bruni, "Influence of the Management Strategy on the Performances of Hybrid Power Systems Integrating Renewable Energy Sources," Doctor of Philosophy (Ph.D.) A dissertation submitted for the degree of Doctor of Philosophy (Ph.D.), Industrial Engineer, Università degli Studi di Roma "Tor Vergata", 2014.



## Hybrid Renewable Systems for Microgrids: Influence of System Sizing on Performances.

BARTOLUCCI LORENZO, CORDINER STEFANO, MULONE VINCENZO, ROCCO VITTORIO & ROSSI JOAO LUIS

**Abstract** In the last years, several works have been presented on the study of the Hybrid Power System (HPS) as effective means of increasing the exploitation of local renewable energy sources in the Distributed Generation (DG) paradigm context. This work aims at thoroughly analyzing the mentioned effects for two different energy demand profiles: an industrial facility and a residential complex of 75 apartments. A parametric analysis with different components sizing was done to evaluate the optimal solution in terms of deployment of renewable energy, resilience of the system and environmental impact, considering the economic convenience as a feasibility constraint. Results show that the two main drivers for the convenience of such systems are the load profile and the PV power plant size. The former shows higher effectiveness of the MG management for the residential load rather than the industrial one. The latter shows that the correct sizing of the PV plant is a better economic solution thanks to a smarter use of the battery and to a lower dependence on the energy exchanged with the EG.

**Keywords:** • Hybrid System • Microgrid • Energy demand • Electric Main Grid • Distributed Generation •

---

CORRESPONDENCE ADDRESS: Bartolucci Lorenzo, Ph.D., University of Rome Tor Vergata, Department of Industrial Engineering, via del Politecnico 1, 00133 Rome, Italy, e-mail: lorenzo.bartolucci@uniroma2.it. Cordiner Stefano, Ph.D., Full Professor, University of Rome Tor Vergata, Department of Industrial Engineering, via del Politecnico 1, 00133 Rome, Italy, e-mail: cordiner@uniroma2.it. Mulone Vincenzo, Ph.D., Associate Professor, University of Rome Tor Vergata, Department of Industrial Engineering, via del Politecnico 1, 00133 Rome, Italy, e-mail: mulone@uniroma2.it. Rocco Vittorio, Ph.D., Full Professor, University of Rome Tor Vergata, Department of Industrial Engineering, via del Politecnico 1, 00133 Rome, Italy, e-mail: rocco@uniroma2.it. Rossi Joao Luis, Ph.D., University of Rome Tor Vergata, Department of Industrial Engineering, via del Politecnico 1, 00133 Rome, Italy, e-mail: joao.luis.rossi@uniroma2.it.

## 1 Introduction

According to [1], the rapid industrialization over the past three decades due to globalization, new technologies and increased household energy consumption of the urban population has resulted in an unprecedented increase of the demand for energy, and in particular electricity. This has led to a big supply-demand gap in the power sector. The scarcity of non-renewable energy resources, rising fuel prices, harmful emissions from the burning of fossil fuels and the need for infrastructure expansion led to an unfeasible or unsustainable situation to meet energy demand. As a way of offering a possible solution, the Decentralized Energy Planning (DEP) has become one of the main alternatives considered. The evolution of the DEP paradigm is directly affected by five main factors, as reported by the IEA [2], and namely the developments in distributed generation technologies, the constraints on the construction of new transmission lines, the increased customer demand for highly reliable electricity, the electricity market liberalization and the concerns about climate changes.

The aim of this work is to provide a reliable design tool capable of analyzing the performance of a microgrid power system from several points of view. In particular, the effects on the Network Operator will be highlighted showing how the employment of the microgrids is beneficial for prosumers and providers. Both economic and technical aspects, as well as environmental considerations, are taken into account in the analysis of the results. In the first part of the work the main assumption and the parameters used for the evaluation of the performance are presented, and then results are discussed for the two case studies.

## 2 Definition of parameters and indexes

Different parameter indexes are defined to analyze the numerical results.

### 2.1 Class Index $I_{size}$

$I_{size}$  is representative of the ratio of the total energy demand obtained by RES and is defined as follows [3]:

$$I_{size} = \frac{E_{load}}{E_{RES}} \quad (1)$$

### 2.2 Self-consumption Index

One of the major benefits of using a microgrid is related to the enhanced capability of consume locally the energy produced by RES. This gives a reduction of the transportation costs and losses with related positive effects on the grid management. The self-consumption index is defined as the ratio of the energy locally consumed from RES and the total energy produced by RES.

$$I_{consumption} = \frac{E_{RES} - E_{sold}}{E_{RES}} \quad (2)$$

### 2.3 Resilience Index

It is defined as a measure of the microgrid to absorb the perturbation and manage the flow although in adverse operating conditions. This index represents the capacity of the FC to cover the power peaks, resulting from the subtraction of the power consumed by the load and the power produced by the PV.

$$\rho = \frac{E_{FC(P_{rated})}}{E_{purchased} + E_{FC}} \cdot \frac{P_{FC}}{P_{load\ max}} \quad (3)$$

### 2.4 Economic Indexes

An economic analysis is crucial to assess the feasibility of hybrid systems. In the energy field affordability, it is based on the savings achieved thanks to efficiency improvements or using a more economical source of energy compared to the cost of energy withdrawn from the grid. The economic indexes used in this analysis were: the net present value (NPV) and the payback period (PBP) that are well described in literature [4].

#### 2.4.1 Discount rate

Base on the study carried out in [5] for the Building Performance Institute Europe (BPIE), the value of 4% was taken as the discount rate.

#### 2.4.2 PV system cost

Costs are considered based exclusively on the initial investment, as maintenance costs over the life cycle (assumed 20 years), in this case, are almost negligible when compared to the initial costs. The efficiency has been considered decreasing of about 1% per year was considered. The initial investment amount for the installation of a photovoltaic system directly depends on the installed power, and thus it has been converted into a cost function interpolating real available data, and obtaining a logarithmic function.

#### 2.4.3 Fuel Cell cost

The ageing of the fuel cell has been taken into account evaluating the equivalent time accounting the number of operating hours ( $n_{operation}$ ) and the number of starts in a year weighed by a factor  $k$  as suggested in the literature [6].

$$n_{eq} = n_{operation} + kn_{starts} \quad (4)$$

The total operating costs for the fuel cell are then:

$$C_{FC} = \frac{C_0 \cdot P_{inst}}{N_h} n_{sq} + \frac{E_{FC}}{H_i \eta_{FC}} C_{comb} \quad (5)$$

In Table 1 the values used in the work are reported.

Table 1 – Cost parameters for the fuel cell

$C_0$ (€/kW)	$N_h$ (h)	$H_i$ (H <sub>2</sub> )	$C_{H_2}$ (€/kg)	$K$ (h)
3000	9500	120MJ/kg	5	3

#### 2.4.4 Battery pack cost

The battery pack costs were evaluated according to the equation:

$$C_{batt} = \frac{C_0 \cdot kWh_{inst}}{N_h} n_h \quad (6)$$

The values of the parameters are reported in [7] and showed in table 2.

Table 2 – Parameters used for the battery pack

$N_h$	$\eta_{charge}$ (%)	$\eta_{discharge}$ (%)	$C_0$ (€/kWh)
2000	90	95	150

#### 2.4.5 Energy from grid cost

Typical electricity costs for the Italy were used (see Table 3) [8], without incentives in accordance with the current legislation.

Table 3 – Time zone costs for both University and Residential facilities

Time zone	University	Residential
F1	0.13 €/kWh	0.21 €/kWh
F2	0.16 €/kWh	0.16 €/kWh
F3	0.15 €/kWh	0.15 €/kWh

The following costs have been considered related to the integration of RES and the Grid:

- Interruption costs [9];
- Replacement and unbalance costs;

- Cycling costs [10];
- Curtailment costs [11].

Based on the work presented in [12], a cost function (Figure 1) depending on the RES penetration has been used in the work to take into account all those aspects.

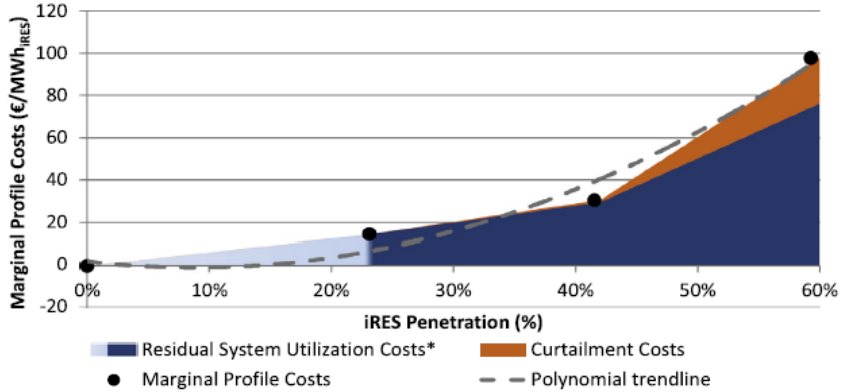


Figure 1 – Cost function over RES penetration [8]

Then the cost for the grid provider due to the presence of the RES has been evaluated according to the following expression:

$$C_{grid\ RES} = C_{interr} + C_{profile} \quad (7)$$

where the profile costs are calculated multiplying the energy fed into the grid by the system times the specific cost value represented in Figure 1.

### 2.4.7 Grid Convenience Index

A grid convenience index has been defined taking as a reference the scenario without RES, evaluating the change in costs for the network operator due to the conversion of renewables with and without a microgrid system.

$$I_{grid} = \frac{C_{grid\ RES} - C_{grid\ RES+MG}}{C_{grid\ RES}} \quad (8)$$

## 2.5 Environmental Index

The avoided CO<sub>2</sub> emissions are evaluated according to the following equation:

$$\Delta e_{CO_2} = e_{grid} \cdot \Delta E_{purchased} + \varepsilon_{grid+conv} \cdot E_{sold} - e_{PV} E_{PV} \quad (9)$$

### 3 Case Studies

Two different cases are analyzed in this work:

- an “industrial-like” facility, in particular the University Industrial Engineering building;
- a residential complex of 75 apartments.

For what concerns the energy demand of the University Industrial Engineering building the real power profile has been considered, while the residential energy demand profile has been generated by means of a stochastic model. The number of apartments has been chosen in order to have a similar amount of the energy demand over a year, although quite remarkable differences of the instantaneous demand profile may arise (Figures 2-3).

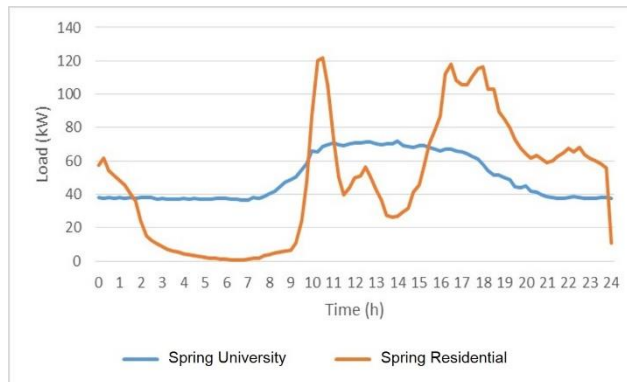


Figure 2 – Reference load profile, Spring.

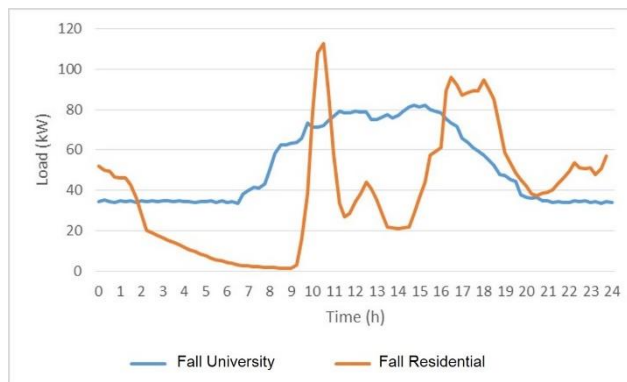


Figure 3 – Reference load profile, Fall.

A sketch of the model used for the residential load generation is reported in Figure 4.

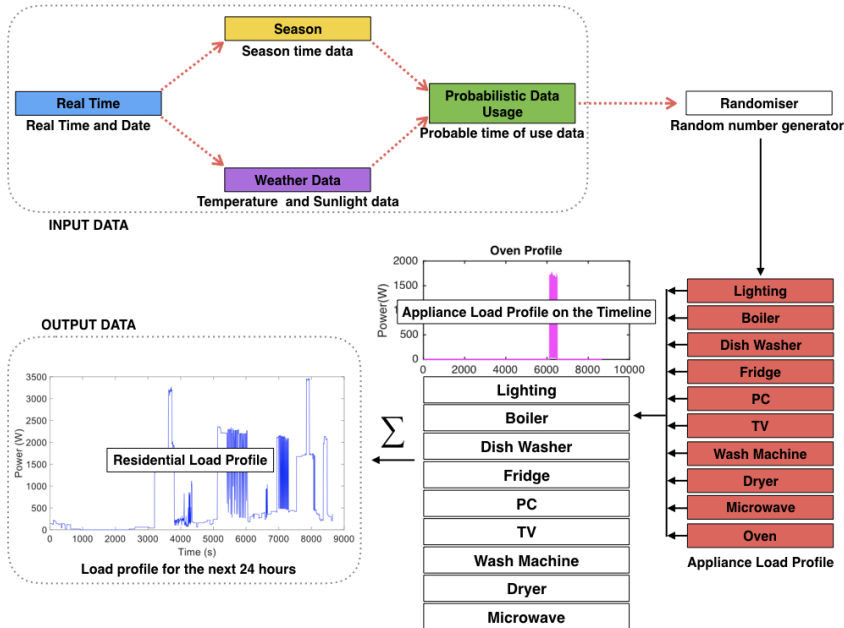


Figure 4 – Load generation model flow chart

Stochastic data have been used as input in a randomizer generating the most probable load profile by means of several parallel simulations, allowing for obtaining reliable energy demand profiles for typical residential facilities located in Rome. Energy consumed by common use appliances have been taken into account, such as: Lighting, Electric Boiler (Shower), Electric Oven, Fridge, Microwave, PC, TV, Dishwasher, Wash Machine and Dryer.

The microgrids for the smart buildings are composed by RES, ESS, FES and grid connected.

The system has been simulated in Matlab-Simulink environment already validated in previous work [13].

#### 4 Results Discussion

The numerical model has then been used to analyze the effect of the components size on the parameters above described for both the industrial and the residential case. Results are presented with respect to the FC and Battery pack sizes, using the class index as an independent sizing parameter.

#### 4.1 Department of Industrial Engineering

Figure 5 shows the energy produced by the fuel cell. It can be noticed that it grows rapidly at the smallest size, saturating towards the greatest values. Moreover, the effect of the battery becomes more evident for higher class index: in fact, a strong decrease in the energy produced by FC is obtained for  $I_{size} = 0.8$  against the highest value of the battery pack, highlighting how using the storage is cheaper than using the FC.

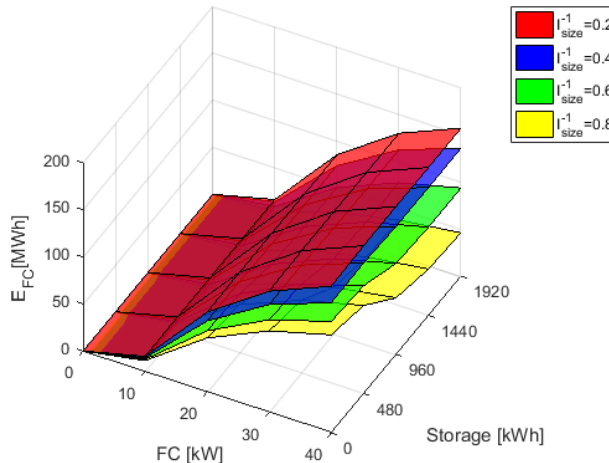


Figure 5 – Energy produced by FC – University case

Figure 6 shows the total energy purchased from the grid: at low  $I_{size}$  the effect of the battery pack is quite negligible while at high  $I_{size}$  a threshold value is obtained above which the increasing battery capacity does not affect the energy exchanged with the grid remarkably.

B. Lorenzo, C. Stefano, M. Vincenzo, R. Vittorio & R. Joao Luis: Hybrid Renewable Systems for Microgrids: Influence of System Sizing on Performances

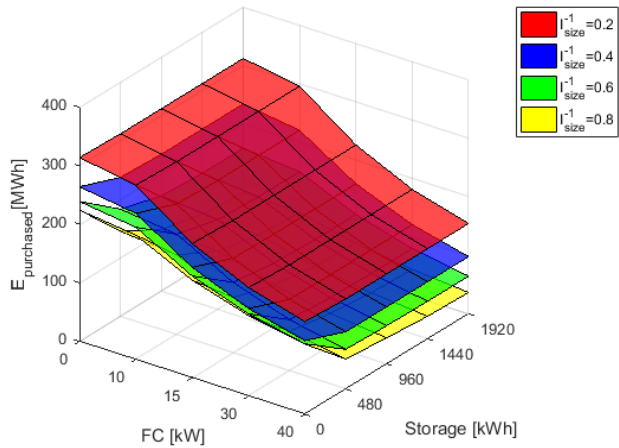


Figure 6 – Energy purchased by the grid – University case

Similar considerations can be drawn looking at the self-consumption index (Figure 7), where a saturation value is presented for the battery pack. The saturation point is clearly increased for the higher-class indexes values, with an evident threshold for the battery pack sizing.

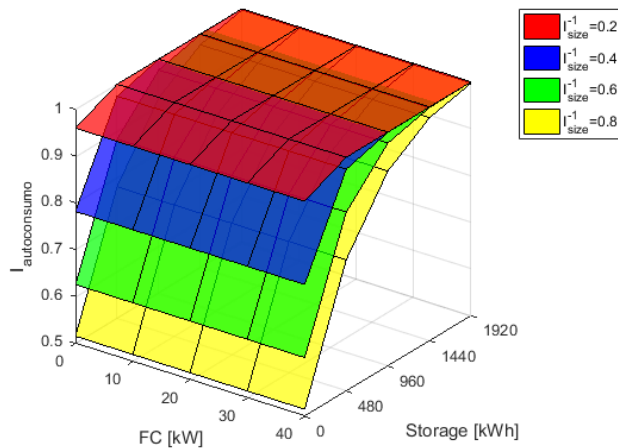


Figure 7 – Self-consumption index – University case

In Figure 8 the resilience index is reported. The index values lower than unity represent a strong grid dependence which is gradually reduced (higher value of  $\rho$ ) by increasing Fuel Cell size. The effect of the battery pack shows again a strong dependence on the class index.

Regarding the grid convenience index, a complex trend is depicted in Figure 9. The effect of the FC is more evident for the lower-class indexes, while for the higher value of the PV sizing, the effect of the battery pack dominates.

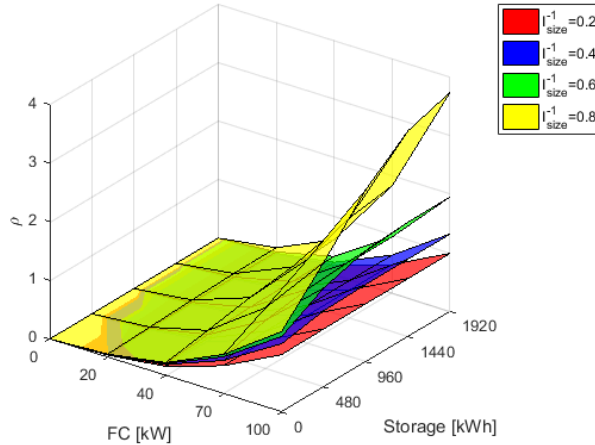


Figure 8 – Resilience index – University case

The capability of the microgrid to store the production in excess, has a positive influence on the grid if compared with the simple use of RES.

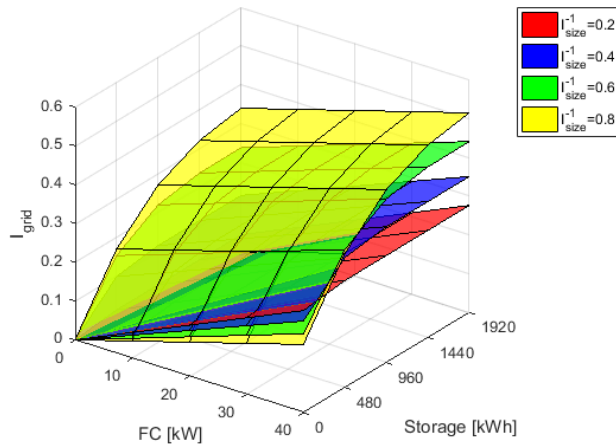


Figure 9 – Grid convenience index – University case

Moreover, positive effects have been obtained in terms of CO<sub>2</sub> emissions (Figure 10).

B. Lorenzo, C. Stefano, M. Vincenzo, R. Vittorio & R. Joao Luis: Hybrid Renewable Systems for Microgrids: Influence of System Sizing on Performances

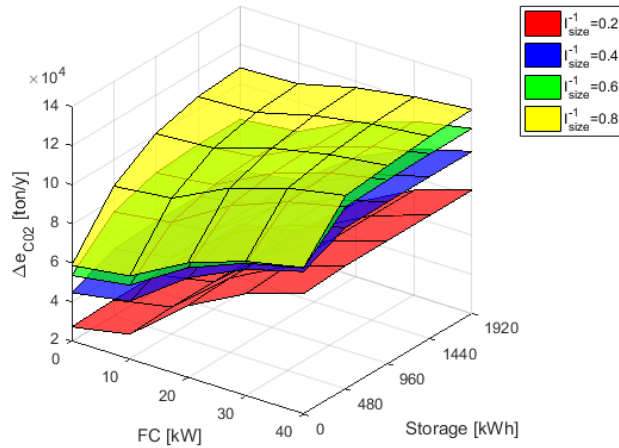


Figure 10 – CO<sub>2</sub> emissions saved – University case

Similar consideration for the effect of the fuel cell use and battery sizing can be drawn, with savings in the range between 1000 and 13000 ton/y.

The NPV analysis (Figure 11) gives negative results for all the simulated cases due to rather low energy costs from the provider, also thanks to the special discount obtained by the university facility management. However, taking into account the beneficial effect on the resilience of the system, on the prosumer-grid interaction and on the environmental index a proper incentivisation strategy could be employed in order to favor the penetration of the microgrid also for this kind of facilities.

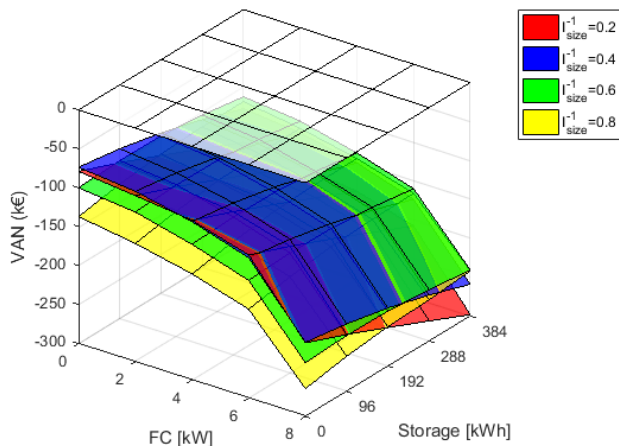


Figure 11 – NPV University case

## 4.2 Residential apartments

Very similar consideration can be drawn looking at the residential case for the energy and environmental indexes. As an example, in Figures 12, 13 the energy purchase and the grid convenience index are respectively reported, highlighting how the influence of the component sizing gets similar to the industrial-like case.

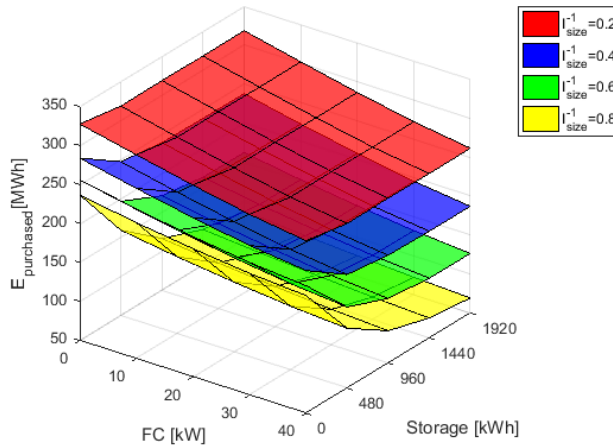


Figure 12 – Energy purchased from the grid – residential case

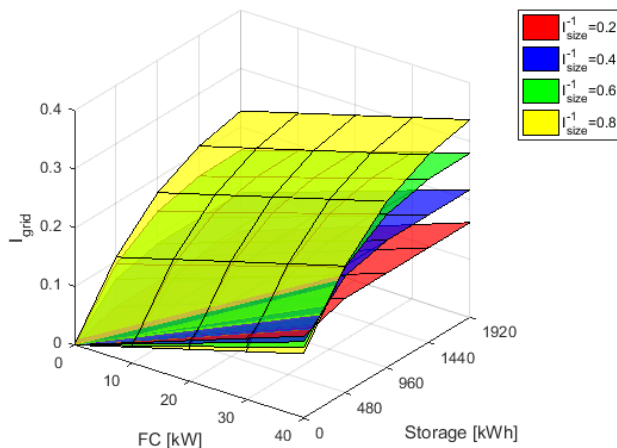


Figure 13 Grid convenience index – residential case

The residential case has thus been considered more interesting. In particular, the convenient economic conditions are reached for low values of the FC sizing (below 9

kW) and for a wide range of PV power output and Battery capacity values (Figure 14). The point of highest interest from the economical point of view is characterized by the highest-class index and medium storage capacity (960kWh). However, taking into account all the aspects mentioned above, different techno-economic optimal aspects can be found in this case.

The PBP (Figure 15) ranges from 5 to 17 years, being strongly affected by the FC sizing; the influence of the battery pack gets less evident whenever the PV sizing is increased. The PV sizing presents less influence, from the economic standpoint, due to the logarithmic function used to define costs.

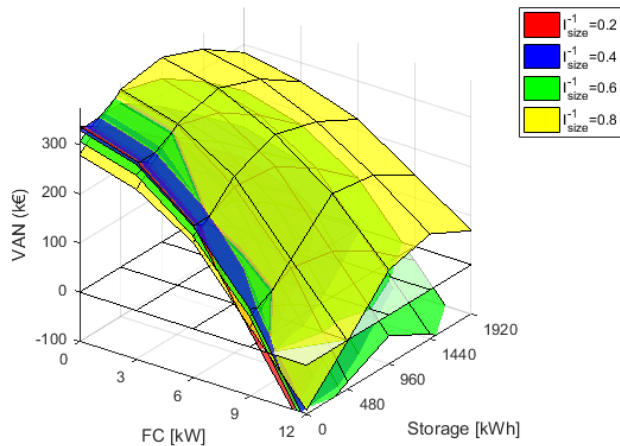


Figure 14 – NPV Residential case

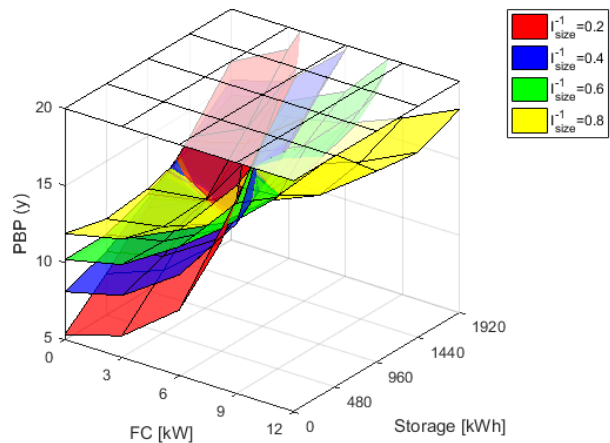


Figure 15 – PBP Residential case

## 5 Conclusions

In this paper a numerical model, previously validated, has been used as a design tool to analyze the performance parameters of a microgrid power system with respect to different aspects. In particular, the effects on the Network Operator have been highlighted showing how the implementation of a distributed energy conversion scenario through microgrids may be beneficial not only for Prosumers side, but also for providers. Economic, technical and environmental aspects have been all taken into account. The following synthetic conclusions can be supported by the results obtained:

- An evident correlation between the PV sizing and battery capacity has been shown, along with a threshold value above which increasing the battery pack becomes less convenient. The threshold value changes with the PV sizing, becoming greater for the higher-class indexes.
- For high values of the battery pack capacities, the influence of the FC decreases highlighting the better convenience of adopting the storage system with respect to a FC system.
- The use of the FC system strongly impacts the resilience of the grid and if coupled with a high battery pack capacity gives a strong grid-independence from the standpoint of prosumers.
- The economical convenience can be achieved more easily in the residential case, as the energy cheap costs would not allow to get positive NPV.
- The PBP ranges between 5 and 17 years in the residential case, and thus a more detailed analysis would be needed to have a more accurate estimation.
- Based on the beneficial effects for the grid provider and in terms of environmental aspects, ad-hoc incentive strategies can be proposed to make the penetration of microgrid systems easier for both the applications proposed.

## Acknowledgements

The authors would like to acknowledge the master students Dario Gesualdi and Lorenzo Sileoni for their valuable contribution to the numerical results commented in this paper and CSF/CAPES (BEX-11965/13-4) – Brazilian Federal Agency for Support and Evaluation of Graduate Education within the Ministry of Education of Brazil.”

## References

- [1] Bajpai, Prabodh, and Vaishalee Dash. "Hybrid renewable energy systems for power generation in stand-alone applications: a review." *Renewable and Sustainable Energy Reviews* 16.5 (2012): 2926-2939.
- [2] IEA 2012 World Energy Outlook
- [3] G. Bruni, S. Cordiner, V. Mulone, V. Sinisi, and F. Spagnolo, "Energy management in a domestic microgrid by means of model predictive controllers," *Energy*, vol. 108, pp. 119-131, Aug 2016.

B. Lorenzo, C. Stefano, M. Vincenzo, R. Vittorio & R. Joao Luis: Hybrid Renewable  
Systems for Microgrids: Influence of System Sizing on Performances

- [4] J. Steinbach and D. Staniaszek, "Discount rates in energy system analysis Discussion Paper," BPIE: Berlin, Germany, 2015.
- [5] Steinbach, Jan, and Dan Staniaszek. "Discount rates in energy system analysis." (2015).
- [6] Chen, Huicui, Pucheng Pei, and Mancun Song. "Lifetime prediction and the economic lifetime of proton exchange membrane fuel cells." *Applied Energy* 142 (2015): 154-163.
- [7] M. Dürr, A. Cruden, S. Gair, and J. McDonald, "Dynamic model of a lead acid battery for use in a domestic fuel cell system," *Journal of power Sources*, vol. 161, no. 2, pp. 1400-1411, 2006
- [8] I. Bertini, B. Di Pietra (ENEA, Technical Unit Energy Efficiency), "The Smart Grid: necessity or opportunity for the future structure of the national power grid," Rome, 2013 (in italian language).
- [9] E. Ghiani, S. Mocci and F. Pilo, "Optimal Reconfiguration of Distribution Networks According to the Microgrid Paradigm," 2013
- [10] NREL, "The Western Wind and Solar Integration Study Phase 2," 2013
- [11] A. S. Brouwer and al., "Impacts of large-scale Intermittent Renewable Energy Sources on electricity systems, and how these can be modeled," 2014
- [12] A. S. Brouwer and al., "Least-cost options for integrating intermittent renewables in low-carbon power systems," 2015
- [13] G. Bruni, S. Cordiner, V. Mulone, Domestic distributed power generation: Effect of sizing and energy management strategy on the environmental efficiency of a photovoltaic-battery-fuel cell system, *Energy*, Volume 77, 1 December 2014, Pages 133-143, ISSN 0360-5442, <http://doi.org/10.1016/j.energy.2014.05.062>.



## Triple Domestic Heat Recovery System: Thermal Modeling and Parametric Study

HASSAN JABER, MAHMOUD KHALED, THIERRY LEMENAND, RABIH MURR, JALAL FARAJA & MOHAMAD RAMADANA

**Abstract** In the last three decades, the domain of heat recovery has been attracting widespread interest. Indeed, it can be seen as a virtual energy source as much essential as renewable sources. That said, many works have been devoted to examine techniques to recover lost heat and optimize the amount of recovered heat. Among the most efficient solution is the use of multi-stages recovery system. The present work suggests a new multi-stage heat recovery system. It combines three heat recovery stages. Heating water, heating air for drying purposes and generating electricity. The concept is applied to exhaust gas of chimney. A complete thermal modeling is presented throughout the paper. Moreover, a case study is carried out for three different types of fuel (diesel, coal, wood). The results reveal that when diesel is used water temperature reaches 351 K and 240 W electric power is generated by TEG. Moreover, 0.0076kg/s of air at 363 K is provided for drying.

**Keywords:** • Heat recovery • thermoelectric generators • thermoelectric cogeneration • dryer • thermal modelling •

---

CORRESPONDENCE ADDRESS: Hassan Jaber, Ph.D. Student, Lab Instructor, Lebanese International University, School of Engineering, PO Box 146404 Beirut, Lebanon, e-mail: hassan.jaber@liu.edu.lb. Mahmoud Khalid, Ph.D, Associate Professor, Lebanese International University, School of Engineering, PO Box 146404 Beirut, Lebanon, e-mail: mahmoud.khalid@liu.edu.lb. Thierry Lemenand, Professor, University of Angers, Angers, 40 Rue de Rennes, 49035 Angers, France, e-mail: thierry.lemenand@univ-angers.fr. Rabih Murr, Ph.D, Assistant Professor, Lebanese International University, School of Engineering, PO Box 146404 Beirut, Lebanon, e-mail: rabih.murr@liu.edu.lb. Jalal Faraj, Ph.D, Assistant Professor, Lebanese International University, School of Engineering, PO Box 146404 Beirut, Lebanon, e-mail: jalal.faraj@liu.edu.lb. Mohamad Ramadan, Ph.D, Assistant Professor, Lebanese International University, School of Engineering, PO Box 146404 Beirut, Lebanon, e-mail: mohamad.ramadan@liu.edu.lb.

## 1 Introduction

In the current days, reducing global energy consumption became a major interest. This interest is caused mainly by high cost of energy sources, high emissions of toxic gases, global warming and obligatory governmental laws. The main sources of energy are fossil fuels which are experiencing rapid increase in their cost. Besides, due to the fact that energy consumption is an effective parameter on the cost of industrial product, alternative energy has gained significant place in scientist researches in addition to maximizing the benefits of wasted energy. [1].

Energy recovery and renewable energy are the perfect solutions for such problems [2]. The concept of renewable energy relies on capturing energy from a natural renewable source like solar, wind, wave, etc. [3-8]. However, energy recovery deals with wasted energy from a facility to the environment. Recovering wasted energy increases the efficiency of the system and reduces pollution as well as cost of energy. This lost energy is mainly released by exhaust gases or cooling water. Many applications have high amount of wasted heat in its exhaust gases and could be recovered like steam boilers, engines, ovens, chimneys, furnaces, etc. [9-18].

To proceed, the present work suggests a heat recovery system that recovers exhaust gases thermal energy to heat domestic hot water, generate electricity and produce hot air that will be utilized in dryer. This system is coupled with a residential chimney in which exhaust gases produced from burning fuel for chimney is utilized to enter a domestic thermoelectric cogeneration drying system.

The design of the system is illustrated in section 2. Then a complete thermal modelling for the system is conducted by applying energy balance at each stage of the system (section 3). Section 4 is devoted for a case study in which different fuels are used and studied, the results were compared, analysed and discussed. Finally, section 5 summarizes main conclusion of the work is done including future work.

## 2 Domestic thermoelectric cogeneration drying system

Figure 1 shows a schematic of thermoelectric cogeneration drying system. Exhaust gases from the chimney pass through a pipe to enter a hybrid heat recovery system and then to a heat recovery heat exchanger to be released to the environment.

This design differs from the conventional system by the two recovery stages: hybrid heat recovery system (HHRS) and heat recovery heat exchanger (HRHE). The main purpose of the hybrid heat recovery system is to absorb part of the thermal energy captured by the exhaust gases to heat domestic hot water and generate electricity. While for the heat recovery heat exchanger, it is utilized to transfer part of the thermal energy of the exhaust gases to heat air which will be transmitted to a dryer for a drying process. Part of thermal energy captured by exhaust gases is released to the HHRS where part of it heats water,

portion generates electricity, and the rest is lost with ambient. Then, another portion of the exhaust gases enters the HRHE where part of the remaining thermal energy on exhaust gases is transferred to heat air.

### 3 System thermal Modeling

In order to study the thermal behavior of the system a thermal modeling is carried at each stage of it. Starting from the combustion of fuel and ending with the released exhaust gases to environment, energy balance is performed and exhaust gases temperature is studied. Besides, water temperature and power generated by TEG at the hybrid heat recovery system are estimated. Finally, impact of changing the mass flow rate of air required for drying on the recovery process is analyzed.

#### 3.1 Furnace

By applying the energy balance at the furnace, the thermal energy released from combustion process through exhaust gases is estimated as follows [19]:

$$\eta_c \cdot Q_f - Q_{L,1} = Q_{gas,1} \quad (1)$$

$$Q_f = \dot{m}_f \cdot LHV \quad (2)$$

where  $Q$ ,  $\dot{m}_f$  are the flow rate (W) and the mass flow rate of fuel (kg/s).  $LHV$  is the lower heating value.

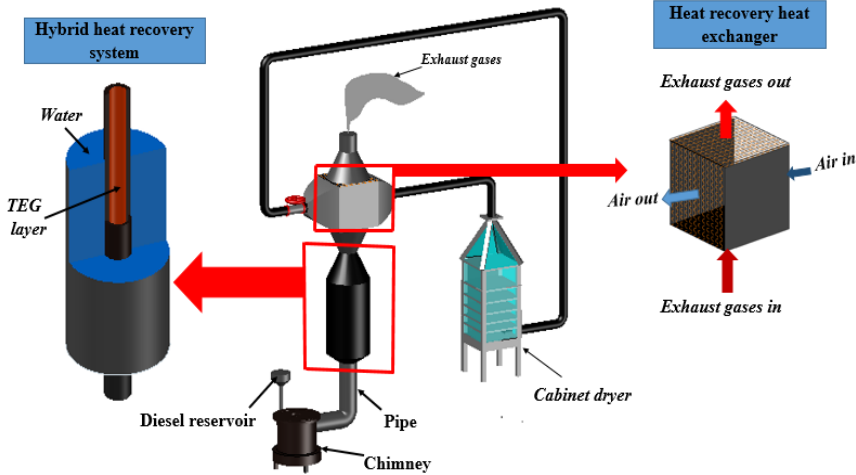


Figure 1. Thermoelectric cogeneration drying system.

The exhaust gases heat rate is function of the quantity ( $\dot{m}_g$ ) and quality ( $T_{g,1}$ ) of exhaust gases

$$Q_{gas,1} = \dot{m}_g \cdot C_{p_g} \cdot (T_{g,1} - T_a) \quad (3)$$

where  $\dot{m}_g$  and  $C_{p_g}$  are the mass flow rate and specific heat at constant pressure of exhaust gases.  $T_{g,1}$  and  $T_a$  are the exhaust gases and ambient air temperatures respectively.

### 3.2 Pipe

By applying energy balance at the pipe shown in figure below

$$Q_{gas,1} - Q_{L,2} = Q_{gas,2} \quad (4)$$

Where  $Q_{gas,2}$  and  $Q_{L,2}$  are the thermal energy hold by exhaust gases at the outlet of the pipe and the lost thermal energy with air respectively. Knowing that the exiting

temperature of exhaust gases from pipe is expressed by  $T_{g,2}$ , the exiting heat rate of exhaust gases is:

$$Q_{gas,2} = \dot{m}_g \cdot C_{p_g} \cdot (T_{g,2} - T_a) \quad (5)$$

The heat loss rate at the pipe is estimated by the following equation, where  $U_p$  is the overall heat transfer coefficient of the pipe and  $A_{p,o}$  is the outer area of the pipe.

$$Q_{L,2} = U_p \cdot A_{p,o} \cdot (T_{m,p} - T_a) \quad (6)$$

$T_{m,p}$  is the average mean temperature at the pipe which is estimated as follows:

$$T_{m,p} = \frac{T_{g,1} + T_{g,2}}{2} \quad (7)$$

### 3.3 HHRS

When exhaust gases get out from the pipe, they enter to the first part of the heat recovery process at which domestic hot water is heated and electric energy is generated using TEGs. At the hybrid heat recovery system, thermal energy which enters the system is splatted in which part of it will be transferred to the TEGs then to water and then to the ambient air ( $Q_{sys}$ ), while the other part will remain captured by the exiting exhaust gases ( $Q_{gas,3}$ ).

$$Q_{gas,2} = Q_{sys} + Q_{gas,3} \quad (8)$$

The heat rate at the exit of the system is associated by the following equation, where  $T_{g,3}$  is the exiting temperature of exhaust gases from the system where  $Q_{L,3}$ ,  $P$  are the heat loss rate with ambient air and the power generated by TEGs.

$$Q_{gas,3} = \dot{m}_g \cdot C p_g \cdot (T_{g,3} - T_a) \quad (9)$$

$$Q_{sys} = Q_{L,3} + P \quad (10)$$

where  $Q_{L,3}$ ,  $P$  are the heat loss rate with ambient air and the power generated by TEGs. At the TEG, the power produced is the difference of the thermal energies at the heat source and sink sides.

$$P = Q_H - Q_C \quad (11)$$

It should be noted that  $Q_H$  is equal to  $Q_{sys}$  and  $Q_C$  is equal to  $Q_{L,3}$ .

Since the max energy conversion efficiency of TEG is about 5%, the TEG layer is represented as a layer having its own thermal resistance with a constant heat flow rate across the system in order to simplify the calculation. In other words, since the power generated ( $P$ ) is very small compared the heat transfer rate across the system ( $Q_{sys}$ ), the heat transfer rate is assumed to be constant over the system allowing to initialize the following equations.

$$Q_{sys} = U_{sys} \cdot A_{t,o} \cdot (T_{m,sys} - T_a) \quad (12)$$

where  $U_{sys}$ ,  $T_{m,sys}$  are the overall heat transfer coefficient of the HHRS and the average mean temperature at the HHRS.  $A_{t,o}$  is the outer area of the tank.

The average mean temperature is function of the entering and exiting exhaust gases temperature from the system:

$$T_{m,sys} = \frac{T_{g,2} + T_{g,3}}{2} \quad (13)$$

The power produced per one TEG ( $P_{1TEG}$ ) is directly proportional to the square of the temperature difference at the TEG ( $\Delta T^2$ ):

$$P_{1TEG} = \left( \frac{P}{\Delta T^2} \right)_{ref} \cdot \Delta T^2 \quad (14)$$

where  $\left( \frac{P}{\Delta T^2} \right)_{ref}$  is the reference ratio of power generated for a specific square of temperature difference provided by the manufacturer.

The total power produced by TEGs ( $P_{total}$ ) is estimated by multiplying the power produced by one TEG with the number of TEGs available at the pipe ( $N_{TEG}$ ).

$$P_{total} = N_{TEG} \cdot P_{1TEG} \quad (15)$$

### 3.4 Dryer

After recovering the first part of energy lost at the HHRS, exhaust gases enter to the second part of heat recovery process in which air is heat to be used in drying process. The outlet air temperature and the mass flow rate of air are suggested in order to calculate the required heat exchange area.

By applying the thermal energy balance at the heat recovery heat exchanger (HRHE) which is shown in figure 8, the following equations are raised:

$$Q_{gas,3} = Q_{HRHE} + Q_{gas,4} \quad (16)$$

$$Q_{gas,4} = Q_{H,HE} = \dot{m}_g \cdot Cp_g \cdot (T_{g,4} - T_a) \quad (17)$$

$$Q_{C,HE} = \dot{m}_a \cdot Cp_a \cdot (T_{a,o} - T_a) \quad (18)$$

$$Q_{H,HE} = Q_{C,HE} = U_{HE} \cdot A_{HE} \cdot \Delta T_{lm} \quad (19)$$

where  $Q_{HRHE}$  is the heat transfer rate to heat exchanger.  $Q_{gas,4}$ ,  $Q_{H,HE}$  and  $Q_{C,HE}$  are the sensible heat rate exiting the heat exchanger, hot and cold stream heat transfer rate at the heat exchanger respectively.  $\dot{m}_a$ ,  $T_{g,4}$  and  $T_{a,o}$  are the mass flow rate of air, exiting exhaust gases and air temperature from the heat exchanger.

## 4 Case study and results

Diesel, coal and wood chimney are the main types of chimneys utilized residentially. They are different in the shape of the furnace (coal and wood include ash drawer) and residues from burning.

### 4.1 Furnace

The three cases will be considered in this study in order to check the effect of changing the fuel used in burning on the behaviour of the double stage hybrid heat recovery system. Table 1 shows each type of fuel with its corresponding lower heat value and a constant mass flow rate of fuel for all types (1.1 kg/hr). For a 60% combustion efficiency the thermal energy generated by burning fuel is also shown in the table below:

Table 1. Lower heat value, mass flow rate and thermal energy of fuel.

Type of fuel	LHV (MJ/kg)	$\dot{m}_f$ (kg/hr)	$\eta_c$	$\eta_c \cdot Q_f$ (W)
Diesel	43.41	1.1	0.6	7958
Anthracite coal	28.74	1.1	0.6	5269
Wood	14.52	1.1	0.6	2662

The table shows that the diesel has the highest lower heating value which implies to high thermal energy generated and high thermal energy carried by exhaust gases. The main parameters utilized in the thermal modelling of the furnace are given in the following table.

Table 2. Main parameters for furnace modelling.

Parameter	Value		Unit
	Furnace surface area ( $A_f$ )	Diesel	
	0.13	0.18	
Convection coefficient of gases ( $h_g$ )	10		$W/m^2.K$
Specific heat of gases at constant pressure ( $Cp_g$ )	1140		$kJ/kg.K$
Convection coefficient of air ( $h_a$ )	20		$W/m^2.K$
Ambient air temperature ( $T_a$ )	298		K

Using those parameters and the equations of the furnace the thermal energy lost with ambient air, and thermal energy captured by exhaust gases are estimated. Knowing that the mass flow rate of exhaust gases is estimated using equation 13. The main results for the furnace part are summarized in the following table.

Table 3. Main results for furnace part

Type of fuel	$\eta_c \cdot Q_f$ (W)	$\dot{m}_g$ (kg/hr)	$T_{g,1}$ (K)	$Q_{gas,1}$ (W)	$Q_{L,1}$ (W)
Diesel	7958	35.31	930	7066	886
Anthracite coal	5269	15.44	1041	3632	1622
Wood	2662	8.64	879	1603	1071

It is shown that the diesel produce the highest quantity of exhaust gases (about 4 times what wood produce) but not the highest temperature. However, even though anthracite coal has the highest exhaust gases temperature but diesel exhaust gases has the highest thermal energy which is dependent on mass flow rate and temperature of exhaust gases. Since coal and wood chimneys are larger in area then the heat lost with ambient air will be higher than for diesel chimney.

## 4.2 Pipe

At the pipe, exhaust gases losses part of their thermal energy to ambient air. The pipe equivalent length is 35 cm including the elbow. The inner and outer radii of the pipe are

5 cm and 5.1 cm respectively. The conduction heat transfer of the pipe which is made of iron is 50 W/m.K. The main results are shown in table 4.

Table 4. Main results from pipe part.

Type of fuel	$R_{total,p}$ (K/W)	$T_{g,2}$ (K)	$Q_{gas,2}$ (W)	$Q_{L,2}$ (W)
Diesel	1.355	899	6609	451
Anthracite coal	1.355	937	3132	509
Wood	1.355	740	1211	378

### 4.3 HHRS

As shown in the design of the HHRS the exhaust gases are in a direct contact with TEG surface. The main parameters of the designed hybrid heat recovery system are summarized in the following table.

Table 5. Main parameters for HHRS thermal modelling.

Parameter	Value	Unit
Length of the system	1	m
Inner radius of the tube	0.05	m
Outer radius of the tube	0.051	m
Inner radius of the tank	0.249	m
Outer radius of the tank	0.25	m
Area of TEG	0.003136	m <sup>2</sup>
Thickness of TEG	5	mm
Number of TEG available	100	Piece
$K_{TEG}$	0.18	W/m.K
$K_{tu}$ (Copper)	401	W/m.K
$K_t$ (Iron)	50	W/m.K
$h_w$	20	W/m <sup>2</sup> .K

Using the thermal modelling equation of the HHRS aforementioned above, the main results of the thermal behaviour of the system are summarized in table 6.

Table 6. Main results obtained for the HHRS.

Type of fuel	$T_{g,3}$ (K)	$Q_{gas,3}$ (W)	$Q_{sys}$ (W)	$P_{total}$ (W)	$T_{w,avg}$ (K)
Diesel	815	5777	832	240	351
Anthracite coal	767	2301	831	240	351
Wood	550	690	521	94	331

The hybrid heat recovery system utilized 12.5% of the energy entering the system when diesel is used to produce hot water and generate electricity. This used energy produced 78 °C hot water and generated 240 W from 100 TEGs. When coal is used 26.5% of the entering energy is utilized producing the same water temperature and power as when diesel is used. While when using wood as a fed fuel of the chimney 43% of the entering energy is transferred to the hybrid heat recovery system producing about 58 °C hot water and generating 94 W electric power from TEG layer.

#### 4.4 Dryer

In this part air to air heat recovery heat exchanger is utilized. There are many types of air to air heat exchanger that can be utilized in this system.

In order to estimate the required heat transfer area of the heat exchanger the outlet air temperature is selected to be equal to 363 K. A range of the mass flow rate of air between 0.0001 kg/s to 0.0076 kg/s has been considered with an increment of 0.0003. The heat exchanger plate is made up of copper of cross sectional area 20\*5 cm. The effect of changing the air flow rate on the exhaust gases temperature, area and number of plates required is being showed below.

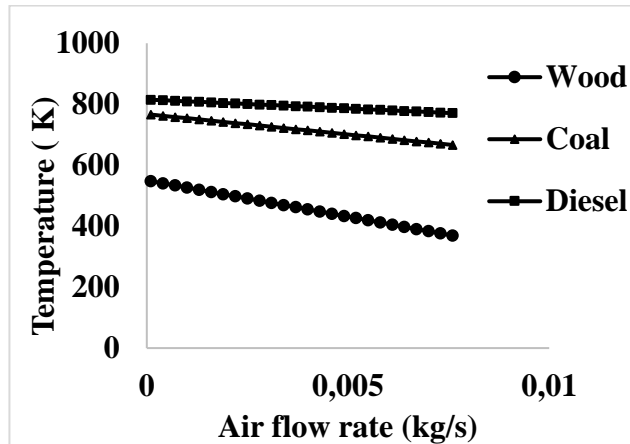


Figure 2. Exiting gases temperature ( $T_{g,4}$ ).

From the figure above it is shown that as the mass flow rate of air is increased the outlet exhaust gases temperature has decreased. The Diesel exhaust gases temperature isn't highly affected by the change of the air mass flow rate, it was 814 K at 0.0001 kg/s and decreased to 770 K at 0.0076 kg/s (decreased 44 degree). This is resulted from the high thermal energy captured by the entering gases. While for the coal exhaust gases, they experienced a 100 degree decrease in temperature while increase air flow rate. Exhaust gases of wood is the most affected by increasing air flow rate. For the available rate the

exhaust gases temperature was 547 K at 0.0001 kg/s and decreased 178 degree at 0.0076 kg/s (369 K).

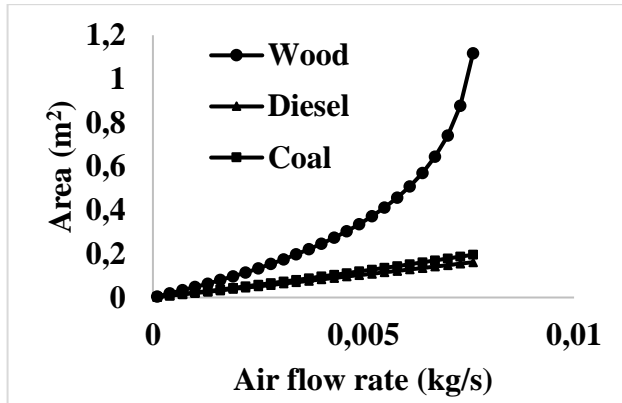


Figure 3. Heat exchanger required area ( $A_{HE}$ ).

The required heat exchanger area is directly affected by changing the mass flow rate. However, as shown in figure 3, diesel and coal are slightly affected compared to the wood case. This is because of the relatively close value of the entering thermal energy of exhaust gases and the required thermal energy to be transfer to air. To illustrate, at a 0.0076 kg/s the area required was 0.16, 0.19 and 1.11 m<sup>2</sup> for diesel, coal and wood respectively.

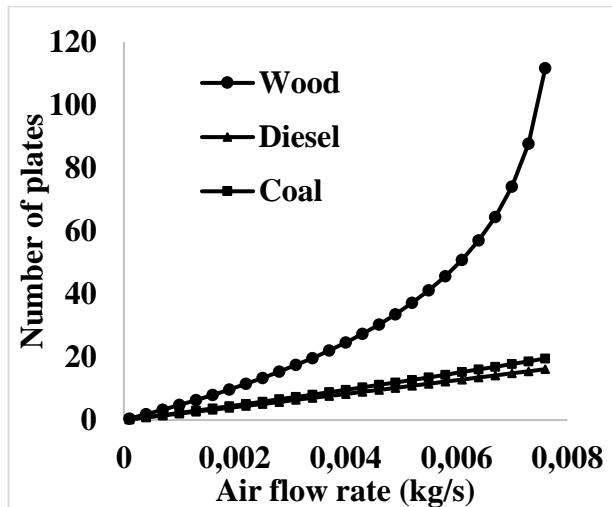


Figure 4. Number of plates required ( $N_{plates}$ ).

The number of plates is proportional to the area, and with constant width and height (20\*5 cm) the change in the number of plate will be as the change in the area. In order of magnitudes, at 0.0076 Kg/s about 17 plate is required when diesel is used and 20 plates for coal and 112 plate when wood is used as the fed fuel of the chimney.

The thermal energy of the exiting exhaust gases is in function of the gases exiting temperature. Figure below shows the effect of changing air flow rate on the energy remaining with exhaust gases.

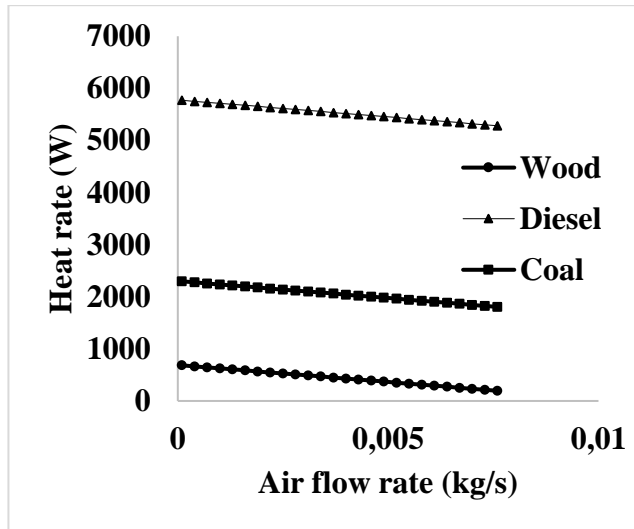


Figure 5. Heat rate at the outlet of the heat exchanger ( $Q_{gas,4}$ ).

From figure 5, at 0.0001 kg/s flow rate of air 6.5 W are released from the exhaust gases to the air. However at 0.0076 kg/s air flow rate, about 500 W of the entering gases are released to air. The energy recovery percentages at the HRHE are summarized in the following table for different fuel used and different air flow rate.

## 5 Conclusion

Multistage heat recovery from exhaust gases is an attractive growing field of study which is capturing the interest of scientists. The present work proposes a new multistage heat recovery system that utilizes thermal energy released from combustion through exhaust gases to heat domestic water, generate electricity and heat air to supply dryer. A complete thermal modeling of the system was illustrated. A case study is conducted in which three types of fuel (diesel, coal and wood) were evaluated. Taken as whole, the results highlight the advantages of the system. At the furnace, significant difference of temperature is

observed depending on the fuel type. For instance, the exhaust gas temperature of coal is 1041 K whereas it is equal to 879 K in the case of wood. By contrast, a mass flow rate of 35.31 kg/hr is obtained for diesel and 8.64 kg/hr for wood. Furthermore, the system provides 240W when coal or diesel are used, in comparison it produces 94 W when wood is utilized. Interestingly, water is heated up to 351 K in the case of diesel and coal, on the other hand when wood is used water temperature reaches 331 K. To supply 0.0076 kg/s of air at 363 K for drying, the required heat exchange surface varies depending on the burned fuel. For instance, 0.16 m<sup>2</sup> is needed for diesel, whereas 1.11 m<sup>2</sup> is required for wood.

## References

- [1] A. Christos, and T. Theochairs, “Energy saving technologies in the European ceramic sector: asystematic review”, *Applied Thermal Engineering*, Vol 21, pp. 1231-1249, 2001.
- [2] D. Zhang, J. Wang, Y. Lin, Y. Si, C. Huang, J. Yang, B. Huang, and W. Li, “Present situation and future prospect of renewable energy in China”, *Renewable and Sustainable Energy Reviews*, Volume 76, , Pages 865-871, September 2017.
- [3] M. Mussard, Solar energy under cold climatic conditions: A review, *Renewable and Sustainable Energy Reviews*, Volume 74, Pages 733-745, July 2017.
- [4] A. Herez, M. Ramadan, B. Abdulhay, and M. Khaled, Short review on solar energy systems, *AIP Conference Proceedings*, Vol 1758, Issue 1 (2016).
- [5] M. Ramadan, M. Khaled, S. Ramadan, and M. Becherif, “Modeling and sizing of combined fuel cell-thermal solar system for energy generation”, accepted in the international journal for hydrogen energy.
- [6] A. Allouhi, O. Zamzoum, M. Islam, R. Saidur, T. Kousksou, A. Jamil, and A. Derouich, “Evaluation of wind energy potential in Morocco's coastal regions”, *Renewable and Sustainable Energy Reviews*, Volume 72, Pages 311-324, May 2017.
- [7] N. Khan, A. Kalair, N. Abas, and A. Haider, “Review of ocean tidal, wave and thermal energy technologies”, *Renewable and Sustainable Energy Reviews*, Volume 72, Pages 590-604, May 2017.
- [8] S. Sharshir, A. Elsheikh, G. Peng, N. Yang, M. El-Samadony, and A. Kabeel, “Thermal performance and exergy analysis of solar stills – A review”, *Renewable and Sustainable Energy Reviews*, Volume 73, Pages 521-544, June 2017.
- [9] H. Jaber, M. Khaled, T. Lemenand, and M. Ramadan, “Short review on heat recovery from exhaust gas”, *AIP Conference Proceedings*, Vol 1758, Issue 1, 2016.
- [10] R. Mal, R. Prasad, and V.K. Vijay, “Renewable Energy from Biomass Cookstoves for Off Grid Rural Areas”, *International Congress on Environmental, Biotechnology, and Chemistry Engineering*, Vol 64, issue 21, 2014.

- [11] R. Carapellucci, and L. Giordano, “The Recovery of Exhaust Heat from Gas Turbines, Department of Mechanical”, Energy and Management Engineering University of L’Aquila Italy
- [12] B. en Zalba, J. Marin, L. F. Cabeza, and H. Mehling, “Review on thermal energy storage with phase change: materials, heat transfer analysis and applications”, Applied Thermal Engineering, Vol 23, 251–283, 2003.
- [13] E. Wang, Z. Yu, H. Zhang, and F. Yang, “A regenerative supercritical-subcritical dual-loop organic Rankine cycle system for energy recovery from the waste heat of internal combustion engines”, Applied Energy, Vol 190, pp. 574-590, 2017.
- [14] A. Mezquita, J. Boix, E. Monfort, and G. Mallol, “Energy saving in ceramic tile kilns: Cooling gas heat recover”, Applied Thermal Engineering. Vol 65, pp. 102-110, (2014).
- [15] M. Wei, W. Yuan, Z. Song, L. Fu, and S. Zhang, “Simulation of a heat pump system for total heat recovery from flue gas”, Applied Thermal Engineering, Vol 86, pp. 326-332, 2015.
- [16] M. Ramadan, M. Gad El Rab, and M. Khaled, “Parametric analysis of air–water heat recovery concept applied to HVAC systems: Effect of mass flow rates”, Case Studies in Thermal Engineering, Volume 6, Pages 61–68, September 2015.
- [17] M. Khaled , M. Ramadan , K. Chahine , and A. Assi, “Prototype implementation and experimental analysis of water heating using recovered waste heat of chimneys”, Case Studies in Thermal Engineering, Vol 5, pp. 127–133, 2015.
- [18] M. Khaled, M. Ramadan, and H. El Hage, “Parametric Analysis of Heat Recovery from Exhaust Gases of Generators”, Energy Procedia, Volume 75, Pages 3295-3300, August 2015.
- [19] Incorpera, F.P. and DeWitt, D.P. 2007. Fundamentals of heat and mass transfer. Sixth Edition. John Wiley & Sons



## **A Wind Park – Pumped Hydro Storage Plant Towards 100% Energy Autonomy for The Island of Sifnos, Greece. Perspectives Created from Energy Cooperatives**

DIMITRIS AL. KATSAPRAKAKIS

**Abstract** The article presents the technical - economic details and the developmental prospects of a wind park - pumped hydro storage plant (PHS), aiming at 100% cover of the electricity needs for the autonomous Aegean Sea island of Sifnos, Greece, following the initiative of the local Sifnos Island Cooperative to claim the island's energy independence and a sustainable social and economic development for the local community.

In the case of Sifnos the target of 100% annual electricity cover from Renewable Energy Sources (RES) can be achievable, given the high available wind potential and the availability of an appropriate site for the installation of a PHS, operating with seawater.

The project's economic feasibility can be ensured with a selling electricity price from the RES – storage power plant of around 0.26 €/kWh, given the high electricity production specific cost (above 0.30 €/kWh) of the existing thermal power plant.

**Keywords:** • wind parks • seawater pumped hydro storage • hybrid power plants • insular remote autonomous communities' development • energy cooperatives •

---

CORRESPONDENCE ADDRESS: Dimitris Al. Katsaprakakis, Associate Professor, Technological Educational Institute of Crete, Faculty of Mechanical Engineering, Estavromenos, 714 10, Heraklion Crete, Greece, e-mail: dkatsap@wel.teicrete.gr.

<https://doi.org/10.18690/978-961-286-049-3.4> ISBN 978-961-286-049-3  
© 2017 University of Maribor Press  
Available at: <http://press.um.si>.

## **1 The Existing Situation in Greece Regarding the R.E.S. Projects Development**

More than 50 remote power systems, located in insular territories, are met in Greece. Currently all the energy needs in the Greek islands are covered by imported fossil fuels, specifically heavy fuel in larger islands for electricity production and diesel oil, almost in all islands, for peak power production and transportation sector. Annual specific electricity production costs range from 0.15 €/kWh in the larger islands to 0.30 €/kWh in smaller ones, while in some cases of very small islands, with some tens of permanent population, this feature may exceed 1 €/kWh.

Another fundamental characteristic of the insular territories in Greece is the rich R.E.S. potential, practically wind potential and solar radiation. Annual averaged wind velocities higher than 10 m/s are often measured in the insular territory [1, 2], while the annual global irradiation is recorded higher than 1,900 kWh/m<sup>2</sup> [3, 4]. The annually available R.E.S. potential in the Greek insular territory outgrows the annual electric [5, 6], thermal and mechanical energy demand and, additionally, can be a fundamental exportable product, capable of becoming the locomotive lever for the recovery of the Greek national economy, starting from the local ones.

Currently, not only the existing R.E.S. potential in the Greek islands remains unexploited, but, in addition, an anarchic policy has been adopted by the investors since 2009. According to the official records of the Regulatory of Authority of Energy (the Authority in charge for the licensing of the submitted R.E.S. projects applications), the total RES projects licensed power exceeds 30 GW, while the annual maximum power demand in Greece ranges around 11 GW.

Another impressive point is the large number of applications and licenses for electricity production projects (mainly wind parks) of very large size (thousands of MWs) in the Greek islands [7], undertaking also the interconnection of the insular systems with the mainland grid through underwater cables for the transportation of the produced power.

In many of the above described applications – licenses there are several violations of the restrictions defined in the national siting plan for the construction of electricity production power plants from R.E.S., aiming at the protection of either environmentally sensitive geographical regions, or sites with special value for the Greek history, civilization and development, such as historical or cultural monuments and areas with distinguished natural beauty and considerable contribution to the local economies (beaches, national parks etc).

Additionally, the siting of these large scale projects in small geographical territories, such as the insular ones, often occupying all the available hills and mountains, certainly affects the existing human activities and turns the traditional insular attitude into an electricity

production industrial area, absolutely affecting tourism, which, in most cases, constitutes the local economies main pylon.

Finally, in case of the exploitation of these large R.E.S. projects from a minority of investors, with the local communities totally absent, all the huge potential social and economic benefits that can be gained from R.E.S. projects in favour of the national economy and the local communities are simply lost [8 – 10].

## 2 The Case of Sifnos Energy Coop

Unlike the above described situation, Sifnos Energy Cooperative (SIC) was established in December 2013, aiming to claim the island's energy independence and to create the prerequisites for a sustainable economic and social development for the local community. These targets are approached with a cluster of actions, containing energy saving measures, especially in tourism sector, introduction of electrical vehicles and demand side management policies. All these measures are plugged in a wind park (WP) – Pumped Hydro Storage (PHS) power plant, which is envisaged to constitute the main support pylon for the approach of the SIC's main targets.

This article presents the basic technical and economic features of the proposed WP – PHS power plant and the prospects expected from its implementation.

### 2.1 The WP-PHS operation algorithm

The proposed WP-PHS aims at the 100% annual electricity production in the autonomous insular system of Sifnos. To approach this target, the adequate dimensioning of the WP-PHS is achieved with the iterative execution of the computational simulation of the system's annual operation, following the operating algorithm described below for every hourly calculation step:

1. The available power production from the wind park  $P_{RES}$  and the power demand  $P_d$  are introduced.
2. The wind park's maximum direct penetration  $P_{RESp}$  is set at 15% versus the current power demand  $P_d$  for security reasons. Consequently:
  - a. If  $P_{RES} > 0.15 \cdot P_d$ , then  $P_{RESp} = 0.15 \cdot P_d$ .
  - b. If  $P_{RES} \leq 0.15 \cdot P_d$ , then  $P_{RESp} = P_{RES}$ .
3. The available storage power  $P_{RESav}$  from the hybrid plant will in any case be:

$$P_{RESav} = P_{RES} - P_{RESp}.$$

4. If  $P_p$  is the pumps total nominal power, then the potential power storage  $P_{st}$  will be:

- a. If  $P_{RESav} > P_p$ , then  $P_{st} = P_p$ .
- b. If  $P_{RESav} \leq P_p$ , then  $P_{st} = P_{RESav}$ .

5. The water volume  $V_p$  that should be pumped in the upper reservoir to store the available power  $P_{st}$  for a time step duration  $t$  is ( $\gamma$  the specific weight of water,  $H_p$  the total pumping head and  $\eta_p$  the pumps' hourly overall averaged efficiency):

$$V_p = \gamma \cdot H_p \cdot P_{st} \cdot t / \eta_p.$$

6. The water volume  $V_h$  that should be removed from the upper reservoir so as the hydro turbines remaining power demand  $P_d - P_{RESp}$  is produced by the hydro turbines for a time step duration  $t$  ( $H_h$  the total water falling water head and  $\eta_h$  the hydro turbines' hourly overall averaged efficiency):

$$V_h = \eta_h \cdot \gamma \cdot H_h \cdot (P_d - P_{RESp}) \cdot t.$$

7. The remaining water volume stored in the upper reservoir after the end of the current time calculation step  $j$  is:

$$V_{st}(j) = V_{st}(j-1) + V_p - V_h.$$

8. Firstly it is checked whether the remaining volume  $V_{st}(j)$  exceeds the reservoir's maximum storage capacity  $V_{max}$ :

- a. If  $V_{st}(j) > V_{max}$ , then:
  - $P_{st} = 0$
  - $P_{sur} = P_{RESav}$
  - $V_{st}(j) = V_{st}(j-1) - V_h.$
- b. If  $V_{st}(j) \leq V_{max}$ , then:
  - $P_{sur} = P_{RESav} - P_{st}.$

when  $P_{sur}$  the power production surplus from the wind park.

9. Secondly it is checked whether the remaining volume  $V_{st}(j)$  becomes lower than the minimum water volume  $V_{min}$  that can be contained in the upper reservoir:

- a. If  $V_{st}(j) < V_{min}$ , then:
  - $P_h = 0$
  - $P_{th} = P_d - P_{RESp}$
  - $V_{st}(j) = V_{st}(j-1) + V_p.$
- b. If  $V_{st}(j) \geq V_{min}$ , then:

$$\begin{aligned}
 P_h &= P_d - P_{RESp} \\
 P_{th} &= 0 \\
 V_{st}(j) &= V_{st}(j-1) + V_p - V_h.
 \end{aligned}$$

where  $P_{th}$  is the power production from the thermal generators in the island's existing thermal power plant. The scope of the dimensioning process is to ensure that this power production from the thermal generators remains constantly null for every time calculation step.

## 2.2 Installation site

The above target is neither obvious nor easy to be achieved. Apart from the proper dimensioning, it depends on two basic parameters that cannot be defined or adjusted by the designer of the hybrid power plant: the available wind potential and the appropriate land morphology for the PHS installation. Just like almost all Aegean Sea islands, Sifnos is gifted with high wind potential and intensive land morphology is several sites, suitable for PHS installation. The low annual rainfall, implying not enough water for the needs of the WP-PHS, is compensated with the use of seawater.

In the case of Sifnos, a site appropriate for the installation of both the wind park and the PHS was found, a fact of high importance regarding the minimization of the project's set-up cost. The sites exhibits excellent wind potential. Indeed after a nine-months measurement period (since July 2016), the averaged wind velocity was measured at 9.8m/s, with rare gusts higher than 30m/s. Yet, the most important feature regarding the wind potential is that during July and August, the high power demand period, the averaged wind velocity was measured at 11.8 and 9.1 m/s respectively, namely there is a coincidence of the available wind potential with the annual peak demand period.

In Figure 1, the wind rose and the Weibull distribution for the wind velocity are presented, based on the gathered measurements from the 10m-height wind mast, installed in the wind parks installation site. Additionally, a 3D wind potential map with the installation position of the five wind turbines is presented in Figure 2.

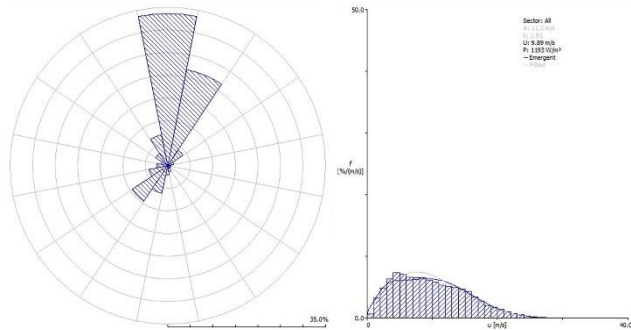


Figure 1: Wind rose and Weibull distribution, based on the wind potential measurements.

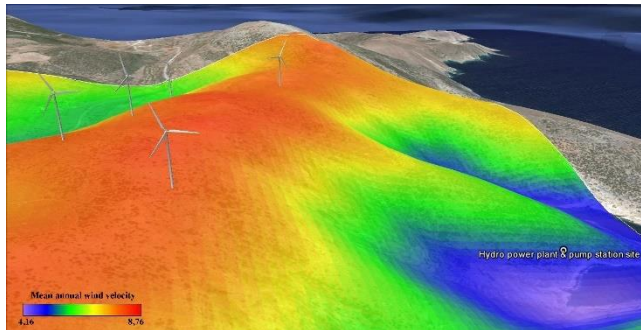


Figure 2: 3D depiction of the wind turbines locations on a wind potential background.

As mentioned previously, the PHS is also installed at the same site with the wind park. A topographic map presenting the overall system's siting on the Greek Coordinates Geodetic Geographical System is given in Figure 3.

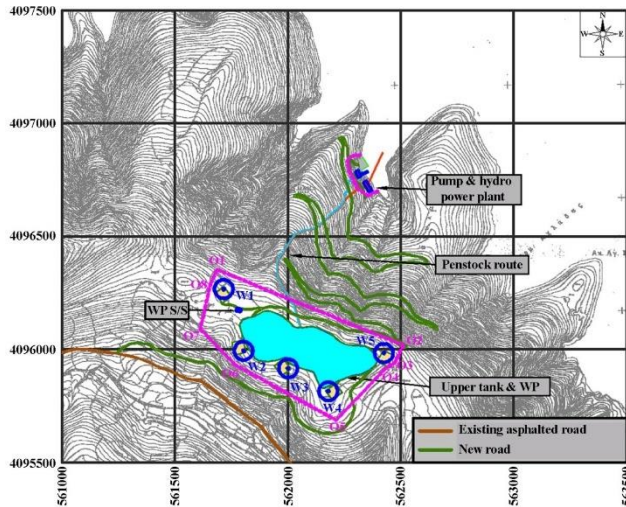


Figure 3: Siting of the WP-PHS.

The upper reservoir of the PHS will be constructed on a ridge with a maximum absolute altitude of 344m. It will follow the shape of the contour of 332m on which the free level of the water surface when the reservoir is full will be.

The maximum depth of the reservoir will reach 20m from the free maximum level of the reservoir, i.e. the bottom of the reservoir at the lower levels will have an absolute altitude of 312m. These dimensions are derived from the morphological characteristics of the area and the requirement for a reservoir construction at the maximum capacity possible, and certainly more than 1,000,000m<sup>3</sup>, taking into account the difference in altitude with sea level (lower tank) and the requirements for guaranteed power.

The total length of the pipeline is 1,183m. The diameter of the pipes will be 2 x 1.00m for the water falling pipes and 2 x 1.00 for the pumping-up pipes, i.e. a double pipeline will be used for pumping up and a double pipeline for the hydraulic drop, in order to secure minimisation of hydraulic flow losses.

### 2.3 Simulation results

The simulation for the Sifnos electrical system was implemented for the year 2020. For this year, the annual electricity consumption in Sifnos is expected to stand at 18,849MWh, while the annual demand peak at 6.526MW. The corresponding curve for the year 2020 resulted from the one of 2015, assuming annual growth of power demand equal to 1.55% for the years 2016-2020.

The final dimensioning is achieved by executing the above described operation algorithm, given the wind potential and the land features presented in the previous section. The results are presented in Table 1.

Table 1. Dimensioning of the WP-PHS

Component	Size
Wind park	5 W/T x 2.3 MW = 11.5 MW
Hydro plant	4 Pelton x 2.185 MW = 8.740 MW
Pumps station	12 units x 902.40 = 10.30
Upper reservoir effective capacity	1,063,878 m <sup>3</sup>
Pipeline diameter	4 x 1.00 m

The WP-PHS operation simulation results regarding the energy production and storage are presented in Table 2. As seen in Table 2, the main goal of the dimensioning, namely the elimination of the thermal generators' production, is achieved. Yet, the resulted dimensioning has led to a considerable annual electricity surplus from the wind park.

Table 2: Annual energy production and storage.

Total energy produced from the wind park (MWh)	35,856.57
Direct energy penetration from the wind park (MWh)	2,135.48
Guaranteed energy produced from the hydro turbines (MWh)	15,518.32
Energy storage from the wind park (MWh)	23,644.30
Energy production from the thermal generators (MWh)	0.00
PHS efficiency (%)	65.63
Wind park energy surplus (MWh)	10,076.78
Wind park energy surplus percentage over the initial production (MWh)	29.88

## 2.4 Economic features

The set-up cost of the WP=PHS is estimated at 37,255,000€. Due to its nature, the investment will try to raise debt finance from the European Investment Bank. For the purposes herein, the loan capital is deemed to be repaid in 15 annual installments with an interest rate of 1.5%. Additionally, the project is anticipated to be funded by the European

Union fourth economic support frame. A possible funding scheme could be 5% private capitals, 45% bank loans and 50% state or EU subsidy.

The investment’s revenues come from:

- the sale of guaranteed electricity
- the sale of guaranteed power.

According to the pricing proposal for the produced guaranteed electricity and the availability of guaranteed power the following shall be applied:

- guaranteed electricity selling price (equal to the existing production cost): **0.2594€/kWh**
- guaranteed power selling price: **188€/kW & year.**

A graphic display of the annual cash flows of the investment is presented in Figure 4. The investment’s economic indices are calculated on the cash flows of net annual profits and the investment’s equities. They are presented in Table 3. The discount rate is assumed at 3%.

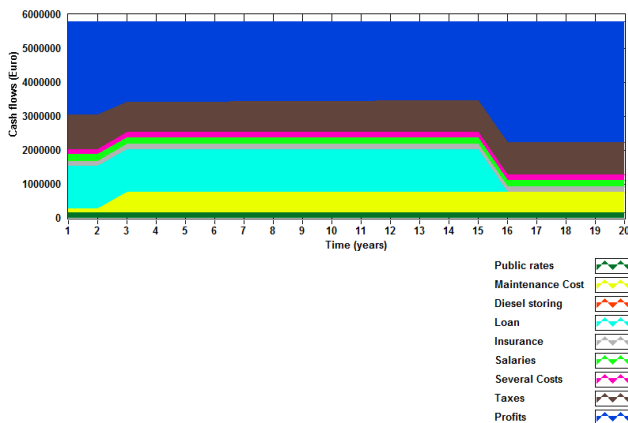


Figure 4: Graphical display of the investment’s annual cash flows.

Table 3: Investment economic indices calculated on the investment's equities.

Net present value (€)	37,503,901.25
Internal rate of return (%)	> 100.00
Equity repayment period (years)	0.68
Equity discounted payback period (years)	0.70
Return on equities (R.O.E.) (%)	2,823.79
Return on investment (R.O.I.) (%)	141.19
Production-specific cost (€/kWh)	0.1281

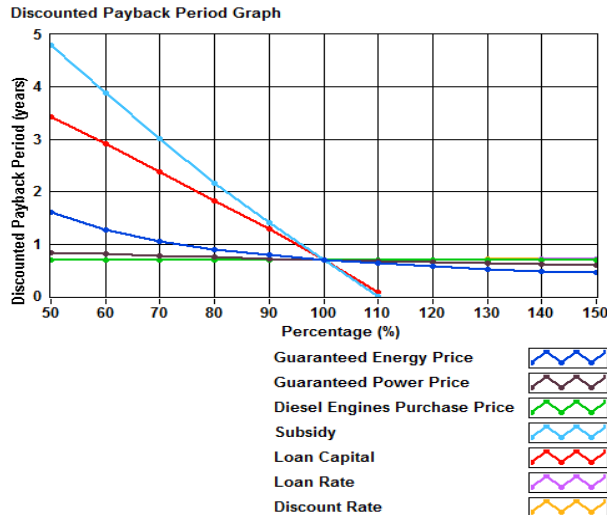


Figure 5: Sensitivity analysis graph of the discounted payback period.

Finally, the sensitivity analysis graph of the discounted payback period is indicatively given in Figure 5, versus several design parameters. From this Figure it is seen that the discounted payback period remains lower than 5 years even if, for example, either the subsidy percentage or the electricity selling price decreases at 50% of the initially assumed values.

### 3 Approaching a Feasible Development Pattern

The construction and the operation of the hybrid power plant will simultaneously lead to a reduction of the annual expenses for the electricity production, currently afforded by the local network operator and to the implementation of a feasible and profitable investment, with an annual net income for the local Energy Cooperation of 3,000,000 €.

Additionally, the potential power surplus from the wind park, estimated at 10 GWh could be exploited in newly introduced loads, such as desalination or electrical vehicles. Adopting an averaged specific electricity consumption for potable water production through a reverse osmosis process of 4 kWh/m<sup>3</sup>, it is estimated that these 10 GWh of electricity surplus, once exploited in desalination units, will permit an annual potable water production of 2,500,000 m<sup>3</sup>. This quantity of available fresh water in a community of 2,500 permanent residents will create a huge potential for the development of new activities in the island, based on the exploitation of the locally available sources and the possibilities offered by the excellent local climate conditions, such as the biological growth of agricultural products and the implementation of pilot farms of biological husbandry, beekeeping etc.

The introduction of these new activities in the island’s local economy will require the disposal of some initial capitals for the construction of the required infrastructure (e.g. potable water storage reservoirs, hydraulic networks, housing of the new enterprises etc). These capitals can be provided by the hybrid power plant’s net profits. Consequently, by re-investing a percentage of the annual net profits of the hybrid power plant for the creation of the required infrastructure, new trades and professions can be introduced in currently unexploited sectors, creating thus serially new occupation positions and strengthening the local economy by introducing additional alternative professional options, instead of the currently economic structure, based almost exclusively on tourism.

Two more major targets of SIC are the transition from conventional transportation means to electrical vehicles within the next 10 years and the procurement of a ship to establish a regular transportation line from Sifnos to Athens, Crete and the largest neighbouring islands (Milos and Santorini), powered either by electrochemical batteries or fuel cells charged by the central WP-PHS. All these actions provide the prerequisites for a secure and sustainable social and economic development of the insular community, with infrastructure and activities based on the locally available energy sources and works with maximized added value.

All this concept is depicted graphically in Figure 6.

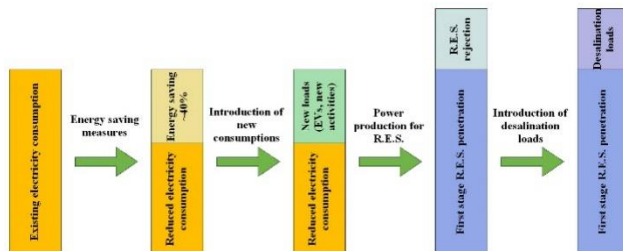


Figure 6: Energy balance between energy saving, energy production from R.E.S. and new loads.

The above fundamental development layout is anticipated by SIC to establish a pattern for all similar insular communities in Greece and worldwide.

### Acknowledgements

Special thanks to the Sifnos Energy Cooperative, for their trust, their contribution and their positive mood.

### References

- [1] Kanellopoulos D., “National wind resources validation in Greece”, *Journal of Wind Engineering and Industrial Aerodynamics*, vol. 39, pp. 367-372, 1992.
- [2] Kotroni V., Lagouvardos K. and Lykoudis S., “High-resolution model-based wind atlas for Greece”, *Renewable and Sustainable Energy Reviews*, vol. 30, pp. 479-489, Feb. 2014.
- [3] Flocas A. A., “Estimation and prediction of global solar radiation over Greece”, *Solar Energy*, vol. 24, pp. 63-70, 1980.
- [4] Photovoltaic Geographical Information System (PVGIS)  
[http://re.jrc.ec.europa.eu/pvgis/cmaps/eu/cmsaf\\_opt/G\\_opt\\_GR.png](http://re.jrc.ec.europa.eu/pvgis/cmaps/eu/cmsaf_opt/G_opt_GR.png)  
(last accessed on 4/4/2017).
- [5] Xydis G., “Comparison study between a Renewable Energy Supply System and a supergrid for achieving 100% from renewable energy sources in Islands”, *International Journal of Electrical Power & Energy Systems*, vol. 46, pp. 198-210, Mar. 2013.
- [6] Katsaprakakis D. Al. and Christakis D. G., “Maximisation of R.E.S. penetration in Greek insular isolated power systems with the introduction of pumped storage systems”, presented at the European Wind Energy Conference and Exhibition 2009, Marseille, 2009, pp. 4918-4930.
- [7] R.A.E. G.I.S. map: <http://www.rae.gr/geo/> (last accessed 3/4/2017).
- [8] Katsaprakakis D. Al. and Christakis D. G., “The exploitation of electricity production projects from Renewable Energy Sources for the social and economic development of remote communities. The case of Greece: An example to avoid.”, *Renewable and Sustainable Energy Reviews*, vol. 54, pp. 341-349, Feb. 2016.
- [9] Silvina Belmonte, Karina Natalia Escalante and Judith Franco, “Shaping changes through participatory processes: Local development and renewable energy in rural habitats”, *Renewable and Sustainable Energy Reviews*, vol. 45, pp. 278-289, May 2015.
- [10] Frank Pieter Boon and Carel Dieperink, “Local civil society based renewable energy organisations in the Netherlands: Exploring the factors that stimulate their emergence and development”, *Energy Policy*, vol. 69, pp. 297-307, Jun. 2014.

## Effect of Fuel Composition Fluctuation on the Safety Performance of an it-SOFC/GT Hybrid System

ZHE CHEN, FENG TIAN, XIAOJING LV, XIAOYI DING & YIWU WENG

**Abstract** Fuel composition fluctuation will cause the system operation to deviate from design condition, especially gasified biomass fuel. Therefore, this work elaborates the safe characteristic and load performance of an intermediate-temperature solid oxide fuel cell (IT-SOFC) and gas turbine (GT) hybrid system using gasified biomass when the composition fluctuates. The malfunction restrictions of components (such as fuel cell thermal crack, compressor surge, reformer carbon deposition) are considered in this research. Results show that the hybrid system has a high efficiency 60.78% at the design point using wood chip gas, which is an interesting reference for distributed power stations. The change of H<sub>2</sub> concentration is most influential to system output power, CO and CH<sub>4</sub> have the similar influence trend. System electrical efficiency increases slightly with the increase of H<sub>2</sub> concentration while decrease significantly with the increase of CO and CH<sub>4</sub> concentration. The system can't operate safely because the turbine is damaged easily by the too high inlet temperature when the H<sub>2</sub> concentration is so high. The carbon deposition is easy to happen in the reformer when the range of moisture content is 0.04~0.38.

**Keywords:** • oxide solid fuel cell • gas turbine • hybrid system • composition fluctuation • safety performance •

---

CORRESPONDENCE ADDRESS: Zhe Chen, Assistant Researcher, Staff of Electric Power Research Institute of Guangdong Power Grid Co., Ltd, Guangdong.510080, China, e-mail: xjjh2006@163.com. Feng Tian, Staff of Electric Power Research Institute of Guangdong Power Grid Co., Ltd, Guangdong.510080, China, e-mail: 44025478@qq.com. Xiaojing Lv, Ph.D, Post-Doctor, Faculty of School of Mechanical Engineering, Shanghai Jiao Tong University, Shanghai 200240, China, e-mail: lvxiaojing@sjtu.edu.cn. Xiaoyi Ding, Ph.D Student in School of Mechanical Engineering, Shanghai Jiao Tong University, Shanghai 200240, China, e-mail: dingxiaoyi\_frank@126.com. Yiwu Weng\*, Professor, Vice President of Energy Research Institute, Shanghai Jiao Tong University, Shanghai 200240, China, e-mail: ywweng@sjtu.edu.cn.

<https://doi.org/10.18690/978-961-286-049-3.5> ISBN 978-961-286-049-3

© 2017 University of Maribor Press

Available at: <http://press.um.si>.

## 1 Introduction

Solid oxide fuel cell and gas turbine (SOFC/GT) hybrid systems are thought to be a promising technology for electric power generation in the future energy markets because of high efficiency, low pollution, and fuel flexibility [1,2].

Biomass is rich and important renewable energy and it has the characteristics of low net CO<sub>2</sub> emission rate and SO<sub>2</sub> emission rate. For this reason, biomass fuelled SOFC/GT hybrid systems are regarded as one of the most attractive power generation equipment [3,4].

For the biomass fuel, the composition and quality depend on the fuel production process and process control parameters used and on the type of biomass that is processed. The gas composition of the biomass gas has significant effect to the performance of the IT-SOFC/GT hybrid system. The main reasons are as follows: 1) fuel cell electrochemical reaction is mainly affected by temperature and fuel composition, and the composition variation will cause a large fluctuation in fuel cell performance [5]; 2) Reforming reactions in reformers are reversible thermodynamic equilibrium [6], which will occur automatically due to the changes in fuel compositions; 3) The combined effect of the previous two factors can cause changes in the thermodynamic performance of other components, and the design and layout of hybrid systems.

Meanwhile a large number of studies have showed that hybrid system may suffer from many S/C constraints in the operations because the H<sub>2</sub>O is essential to the CH<sub>4</sub> reforming reaction and proper H<sub>2</sub>O can avoid carbon deposition. Excess water will increase the cost due to its pressurizing and heating, and it also lowers the SOFC efficiency by diluting the fuel [7]. Another important factor, the amount of water varied will make the hybrid system operate under different moisture environmental conditions, which leads to an important impact on operating characteristics of hybrid system and components (such as fuel cell, reformer, gas turbine).

In this paper, a detailed model of the IT-SOFC/GT hybrid system was established using wood chip gas as fuel. The effects of variable fuel composition and water/carbon ratio on the performance of the hybrid system were studied. The safety performance of the hybrid system was analysed under the safety restrictions such as the fuel cell temperature gradient, the safe surge zone of the compressor and the inlet temperature of the turbine. The results can provide support for the design and application of biomass gas-fuelled hybrid power system.

## 2 IT-SOFC/GT Hybrid System Structure and Mathematical Model

### 2.1 IT-SOFC/GT system structure

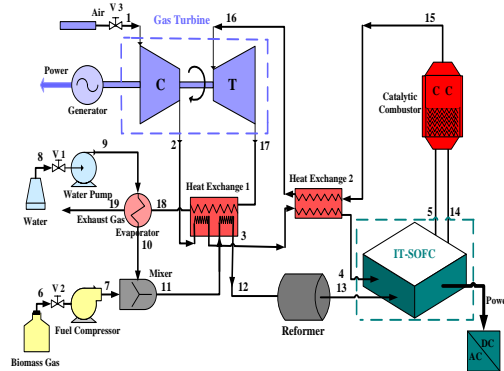


Fig.1. Schematic of IT-SOFC/GT hybrid system

A schematic of the IT-SOFC/GT hybrid system is shown in Fig. 1, which mainly includes IT-SOFC, single-shaft GT, external reformer, catalytic combustor (CC), fuel compressor, water syringe pump, generator, and other components. The water is added for maintaining the ratio of steam to carbon by adjusting valve 1. To prevent seal and vibration caused by the pressure difference between anode and cathode in the fuel cell, biomass gas needs to be compressed by a fuel compressor before entering the fuel cell for electrochemical reaction, which is adjusted by valve 2. Air pressurized by the compressor is heated by heat exchangers (HE) 1 and 2, which then enters the SOFC cathode to provide  $O_2$  for electrochemical reaction (Eq. (1)). Water is first heated in the evaporator to be converted into steam and then mixed with biomass gas in the mixer. The mixed gas enters the reformer after being heated by HE 1. Reformed gas enters the anode to provide  $H_2$ . The unreacted fuel from the SOFC anode will be completely combusted in the CC. High-temperature gas enters the turbine to generate power after heating air. The exhaust gas of the turbine preheats fuel and air, and then heats the evaporator before being released into the atmosphere.



### 2.2 IT-SOFC/GT mathematical mode

The mathematical model of the IT-SOFC/GT established in this study was described in detail in the previous literature [8-10].

In this model, the anode-supported IT-SOFC (873–1073 K) developed by Aguiar [11] is used to fit into the hybrid system. The 2D fuel cell model includes an electrochemical

model and a thermodynamic model based on mass and energy balance equations. The fuel cell stack is assumed to have 912 planar fuel cells, providing 144 kW power.

The gas turbine model is mainly composed of a centrifugal compressor and radial turbine. It is represented by the characteristic maps of compressor and turbine [12,13].

The reforming model is established according to Gibbs free energy thermodynamic equilibrium reaction, mainly including strong endothermic steam reforming reaction and weak exothermic water gas shift reaction.

The hybrid system also includes other components, such as CC, HE, mixer, and syringe pump. The establishment of the models and parameters selection based on energy and mass balance equations can be found in [8,9]. This work assumes that unreacted fuel is completely combusted in the CC.

The hybrid system electric efficiency is:

$$\eta_{HS} = \frac{P_{SOFC} \times \eta_{DC/AC} + (P_T - P_{C,air}) \eta_g \times \eta_m - (P_{C,fuel} / \eta_e) - (P_{P,water} / \eta_e)}{(y_{CH_4}^0 \times LHV_{CH_4}^0 + y_{H_2}^0 \times LHV_{H_2}^0 + y_{CO}^0 \times LHV_{CO}^0) \times M_{fuel}} \quad (2)$$

In this work, the wood chip gasified gas is chosen as the fuel, which is composed of 4.53% CH<sub>4</sub>, 23.64% H<sub>2</sub>, 13.87% CO, 17.92% CO<sub>2</sub> and 40.04% N<sub>2</sub>. The composition of this gasified gas is obtained through the experiment of the two-stage gasification developed by Institute of Thermal Engineering, Shanghai Jiao Tong University. In addition, we also cited the specific constraints for components safety to evaluate the hybrid system performance [8,9].

### 3 Results and Discussions

#### 3.1 System performance of IT-SOFC/GT hybrid system

The operation performance at designed condition is obtained by using above established IT-SOFC/GT mathematic models, as shown in Table 1. It can be observed that designed fuel flow rate is 2.269 mol/s, and all characteristic parameters of main components meet the requirements in Table 3 in [9].

The fuel cell operating parameters coincide with the results from reference [11]. For the small power system designed in this work, the electrical efficiency is 60.78%. It is noted that the catalytic combustor temperature is not more than 1200K and changes homogeneously, causing NO<sub>x</sub> emission to be very low (nearly zero) [12] and CO to be converted into CO<sub>2</sub> completely. Above results show that the hybrid system has good emission and operation performance.

Z. Chena, F. Tiana, X. Lvb, X. Dingb & Y. Weng: Effect of Fuel Composition Fluctuation on the Safety Performance of an it-SOFC/GT Hybrid System

Table 1. Performance of the IT-SOFC/GT Hybrid system.

Type	WCG U <sub>f</sub> =75%
Fuel flow rate/mol/s	2.269
IT-SOFC current density/ A/m <sup>2</sup>	5000
IT-SOFC working temperature/K	1073
IT-SOFC MTG/ K/cm	6.571
S/C boundary value	1.87
IT-SOFC voltage/V	0.79
IT-SOFC power/kW	144.4
TIT /K	1173
Gas flow rate/ kg/s	0.2747
GT power/kW	38.01
Air compressor consumption/kW	27.48
Fuel compressor consumption/kW	7.929
Syringe pump consumption /kW	0.012
Hybrid system power/kW	182.4
Hybrid System efficiency/%	60.78

### 3.2 Effect of biomass gas compositions on system performance

As the raw materials of biomass gas varies from each other greatly in sources and properties, the composition of biomass gas will usually change, resulting in deviation from the design operating system condition. The performance of the hybrid system was studied with biomass gas concentration (CO, H<sub>2</sub>, CH<sub>4</sub>) changing in the range of -20% to + 20% from the design concentrations while the current density and the fuel flow rate are constant, (Note: In the calculation, when the composition of one effective fuel changes, the others components in the remaining volume stay the initial proportion unchanged). The effect of each component change on the performance of the hybrid system is shown in Figures 4-6.

As can be seen from figure 4, the working temperature and voltage of fuel cell both increase with the increase of the fuel concentration. It is also found that when fuel concentration increases, ohmic polarization and electrode polarization resistance decrease while the Nernst potential of the battery rises, resulting in the fuel cell output voltage increases. It can also be seen from the figure that, percentage changes of H<sub>2</sub> has the largest effect on battery performance parameters, while CH<sub>4</sub> the minimum, this is related to the proportion of the various components in the biomass gas.

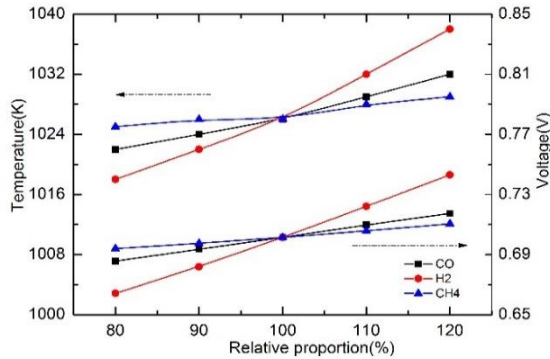


Fig. 4 Fuel cell working temperature and voltage variation

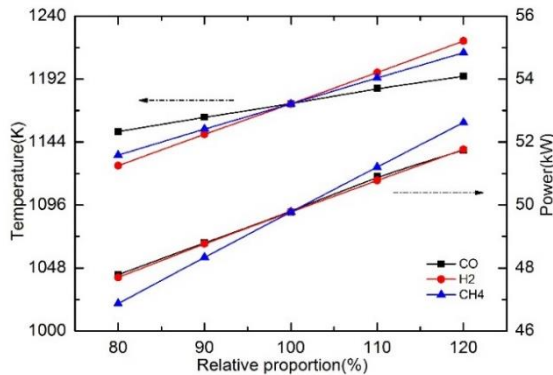


Fig. 5 Turbine inlet temperature and output power variation

Figure 5 shows the effect of fuel concentration on turbine inlet temperature and output power. It is found that both the turbine inlet temperature and the gas turbine output power increase with increasing percentage of each component. This is because the amount of combustible components entering the catalytic combustion chamber is increased and more heat is released, making turbine inlet temperature increase. And the increase of H<sub>2</sub> percentage has the largest effect on turbine inlet temperature. It can also be seen that the change in the output power of the gas turbine is almost the same when the percentage of H<sub>2</sub> and CO is varied.

Z. Chena, F. Tiana, X. Lvb, X. Dingb & Y. Weng: Effect of Fuel Composition Fluctuation on the Safety Performance of an it-SOFC/GT Hybrid System

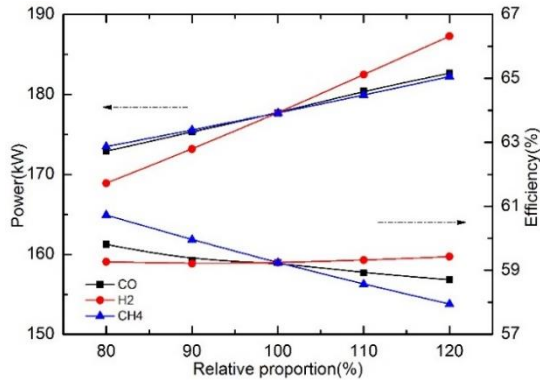


Fig. 6 System output power and electrical efficiency variation

It can be seen from Figure 6 that the output power of the system increases with the increase of the components, and the variation range affected by H<sub>2</sub> percentage is the biggest, while the change of CO and CH<sub>4</sub> percentage has relatively smaller effect. The power generation efficiency of the system increased slightly with the increase of H<sub>2</sub> percentage and decreased with the increase of CO and CH<sub>4</sub> percentage. This is due to that fuel cell accounts for the main part of the output power of the hybrid system.

When the composition of the biomass gas is changed, the system operating parameters are within the requirements of Table 3 in [9], which means the system can be operated safely. As can be seen from the results, the appropriate reduction in CH<sub>4</sub> percentage or increase of H<sub>2</sub> percentage are benefit to improving system performance.

### 3.3 Effect of moisture content on system performance

In this research, the moisture content entered the system is calculated by the corresponding formulas according to the value of S/C varied from 0.5 to 4.5.

The water amount variation changes the fuel composition concentration, which leads to the fuel cell electrode kinetics and thermodynamics change [14]. The moisture content of fuel cell exit calculated changes from 0.08 to 0.34, which lead to the variation of fuel cell characteristic, as shown in Figs.7-8.

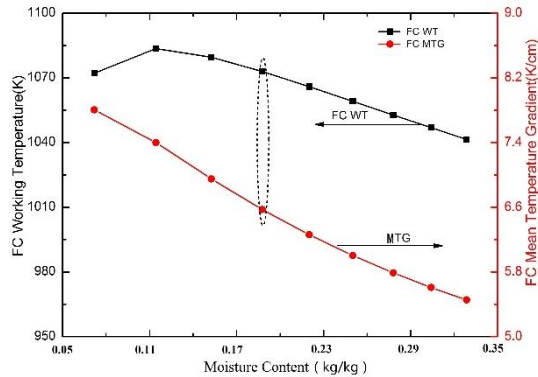


Fig.7. Fuel cell WT and MTG

Figure.7 shows that the fuel cell working temperature has a maximum value 1083K when the moisture content is equal to 0.12, and then decreases from 1083K to 1041.46K with increasing water. This is because that, when the current density is constant, the heat released by the fuel cell electrochemical reaction will not be changed. The increasing water causes more heat to be absorbed by  $\text{CH}_4$  steam reforming and increases the cooling effect from  $\text{H}_2\text{O}$  on the fuel cell stack. Obviously, the MTG decreases linearly from 7.80K/cm to 5.45 K/cm, which is within the safe operation range shown in Table 3 in [9].

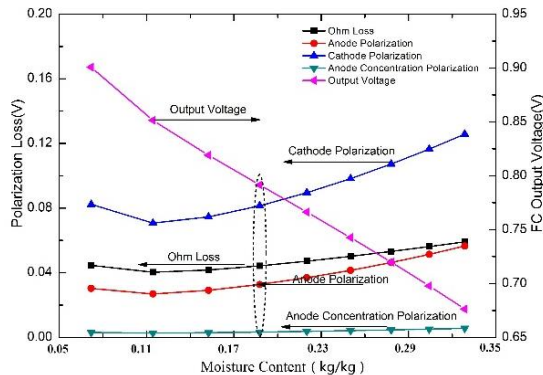


Fig.8. Fuel cell polarization loss and voltage

Figure.8 shows that fuel cell output voltage decreases and the polarization losses of fuel cell anode, cathode and ohm increase with increasing water. It also can be seen, for the various polarization losses of the selected fuel cell, the polarization losses of cathode and ohm occupy the main part. This result is consistent with the variation trend of the voltage and polarization losses in the reference [11].

Z. Chena, F. Tiana, X. Lvb, X. Dingb & Y. Weng: Effect of Fuel Composition Fluctuation on the Safety Performance of an it-SOFC/GT Hybrid System

The characteristics of reforming is mainly decided by the reactor temperature (exit temperature), fuel composition, reaction pressure and the amount of water entered the reformer. The moisture content of reformer exit calculated changes from 0.04 to 1.02, which lead to the variation of reformer characteristic, as shown in Figs.9

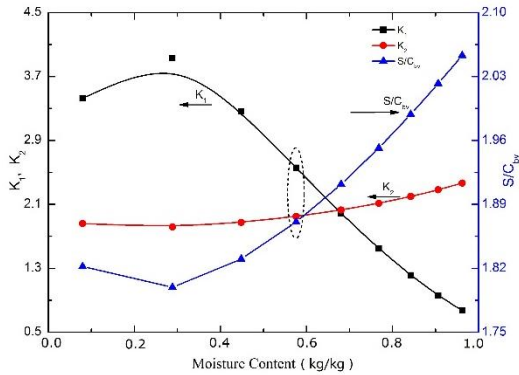


Fig.9.  $K_1$ ,  $K_2$  and  $S/C_{bv}$

In reforming process, the increasing reaction equilibrium constant  $K_i$  means that the forward reaction is performed, vice versa. Figure 9 shows that the  $CH_4$  reaction equilibrium constants  $K_1$  has a peak value 3.93 and then decreases to 0.77, while the  $K_2$  increases from 1.86 to 2.87 lineally. It also can be seen, the  $S/C_{bv}$  decreases at first and then increases with the increasing water. When the water added in the reformer is higher than the  $S/C_{bv}$  value required, the carbon deposition is can be effectively prevented at least in theory. When the range of moisture content is 0.04 ~0.38, the carbon deposition easily occurs because the water is not enough for the reforming reactions. In this condition,  $CH_4$  and CO cracking reactions may be accompanied by  $CH_4$  reforming reaction, leading to carbon deposition, which can plug gas diffusion pores and weaken the activated catalyst, and finally causing the performance of reformer to deteriorate.

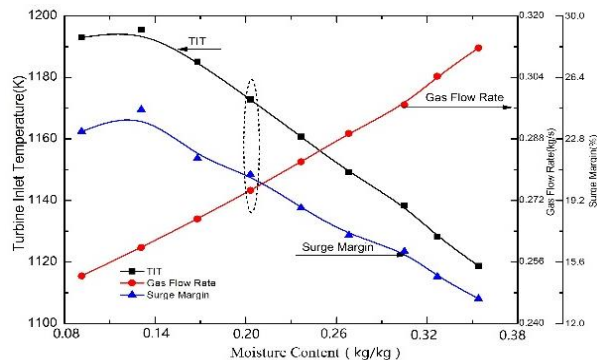


Fig. 10. TIT, gas flow rate and surge margin

In the hybrid system, the mass fraction of water entered the turbine increases from 8.26% to 25.77% with the variation of S/C, the corresponding moisture content changes from 0.10 to 0.35. Under this condition, the dry combusted gas becomes wet combusted gas[15].

Figure.10 shows that variation trend of TIT, wet gas flow rate and surge margin with moisture content. The TIT has a maximum value at moisture content of 0.12 and then decreases. This is mainly caused by the reaction characteristic of reformer. It also can be seen, the operation point is close to the surge boundary, and the SM decreases from 24.51% to 13.46%. However, the SM of all the operation points is greater than 12% shown in [9], which indicates that the safety requirement is met.

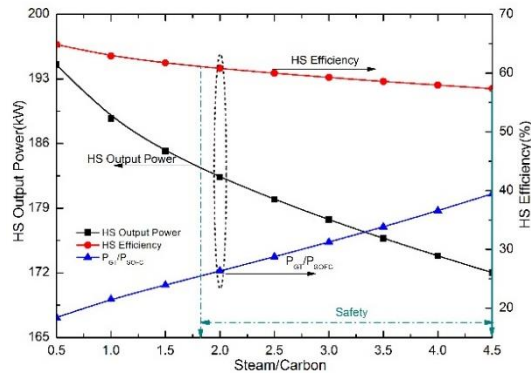


Fig. 11. Performance of the hybrid system

Figure. 11 shows that the power and electrical efficiency of the hybrid system decrease with growing S/C ratio, while the  $P_{GT}/P_{SOFC}$  increases. In the hybrid system,  $P_{GT}/P_{SOFC}$  is an important parameter in the generation performance. It defined as the ratio of power produced by the gas turbine to the power produced by the gas turbine. The bigger the ratio, the smaller the system efficiency. In this calculation,  $P_{GT}/P_{SOFC}$  increases with the increase of the water vapor, which means that the SOFC power covers a smaller proportion in the hybrid system. And the decrease of the fuel cell power is greater than the increase of the gas turbine power with the increase of steam. Therefore, both the hybrid system power and electrical efficiency decrease.

It can be found in the calculation results that when the amount of water vapor is very small (when the S/C is lower than 1.68 in this research), the hybrid system has a good performance, but in this condition, carbon deposition easily occurs in the reformer

#### 4 Conclusions

In this work, using wood chip gasified gas as fuel, the performance of an IT-SOFC/GT hybrid system is analysed, and the effects Fuel composition on the safety performance

and load performances of hybrid system under the consideration of fuel cell temperature gradient, compressor surge zone and turbine inlet temperature are studies. The main conclusions can be drawn, as follows:

1) The IT-SOFC/GT hybrid system of 182.4kW has a high electric efficiency of 60.78% fuelled by wood chip gasified gas. This hybrid system is with very low NO<sub>x</sub> and CO emission, and has good operating performance.

2) The percentage change of H<sub>2</sub> in wood chips gas causes the biggest change of the output power of the system, and the electrical efficiency increases slightly with H<sub>2</sub> percentage increases. Change of CO and CH<sub>4</sub> percentage has little effect on the output power with similar trend, while electrical efficiency of the system decreases significantly with the percentage of CO and CH<sub>4</sub> increasing. The turbine is damaged easily by the too high inlet temperature when the H<sub>2</sub> concentration is so high.

3) With the increase of moisture content, the fuel cell working temperature and mean temperature gradient does not exceed the safety limit value. When the range of moisture content is 0.04~0.38, the carbon deposition is easy to happen in the reformer. With the decrease of water, the performance of the hybrid system improves significantly. But for considering the safe operation for reformer, maintaining a high value of the water is very important.

### Acknowledgements

The research is supported by National Natural Science Foundation of China under grant No. 51376123, Enterprise project of Guangdong Power Grid Co., Ltd under grant No. 036100QQ00160001-001, and Shanghai Sailing Program under grant No.17YF1409800.

### References

- [1] Fuel Cell Handbook. U.S. Department of Energy, Office of Fossil Energy, National Energy Technology Laboratory, November 2004.
- [2] Kaneko T, Brouwer J, Samuelsen G.S. Power and temperature control of fluctuating biomass gas fueled solid oxide fuel cell and micro gas turbine hybrid system. *J Power Source* 2006; 160: 316–325.
- [3] Bang-Møller C, Rokni M. Thermodynamic performance study of biomass gasification, solid oxide fuel cell and micro gas turbine hybrid systems. *Energy Convers. Manage* 2010; 51: 2330-2339.
- [4] Bang-Møller C, Rokni M, Elmegaard B. Exergy analysis and optimization of a biomass gasification, solid oxide fuel cell and micro gas turbine hybrid system. *Energy* 2011; 36: 4740-4752.
- [5] Zabihian F, Fung A S. Performance analysis of hybrid solid oxide fuel cell and gas turbine cycle: Application of alternative fuels. *Energy Convers. Manage* 2013; 76: 571–580.
- [6] Sucipta M, Kimijima S. Biomass Solid Oxide Fuel Cell-Microgas Turbine Hybrid System: Effect of Fuel Composition. *J Fuel Cell Sci Tech* 2008;5.

- [7] Zhang X, Wang Y, Liu T, Chen J. Theoretical basis and performance optimization analysis of a solid oxide fuel cell-gas turbine hybrid system with fuel reforming. *Energy Convers. Manage* 2013; 61:1102–1109.
- [8] Lv X, Lu C, Wang Y, Weng Y. Effect of operating parameters on a hybrid system of intermediate-temperature solid oxide fuel cell and gas turbine [J]. *Energy*, 2015, 91: 10-19.
- [9] Lv X, Liu X, Gu C, Weng Y. Determination of safe operation zone for an intermediate temperature solid oxide fuel cell and gas turbine hybrid system [J]. *Energy*, 2016, 99: 91-102.
- [10] Lv X, Gu C, Liu X, Weng Y. Effect of gasified biomass fuel on load characteristics of an intermediate-temperature solid oxide fuel cell and gas turbine hybrid system [J]. *International Journal of Hydrogen Energy*, 2016, 44:9563–9576.
- [11] Aguiar P, Adjiman C S, Brandon N P. Anode supported intermediate temperature direct internal reforming solid oxide fuel cell. I: Model-based steady-state performance. *J Power Source* 2004.;138:120-136.
- [12] Liu A, Weng Y. Numerical simulation of fuel cells/gas turbine hybrid power system and catalytic combustion experiment study[D]. Shanghai Jiao Tong University PhD. 2009(In Chinese).
- [13] Li Y, Weng Y. Off-design analysis and experiment study of high temperature fuel cell/gas turbine hybrid system[D]. Shanghai Jiao Tong University PhD. 2011 (In Chinese).
- [14] *Fuel Cell Handbook*, Seventh Edition, EG&G Technical Services, Inc. USA, 2004.
- [15] H.I.H. Saravanamuttoo, G.F.C. Rogers, H. Cohen. *Gas Turbine Theory*, Fifth edition, Longman, UK, 2001.





 **energetika** *ljubljana*



 **energetika** *ljubljana*



 **energetika** *ljubljana*



 **energetika** *ljubljana*



 **energetika** *ljubljana*



 **energetika** *ljubljana*



 **energetika** *ljubljana*



 **energetika** *ljubljana*



 **energetika** *ljubljana*



 **energetika** *ljubljana*